World Journal of Stem Cells

Submit a Manuscript: https://www.f6publishing.com

World J Stem Cells 2024 June 26; 16(6): 670-689

DOI: 10.4252/wjsc.v16.i6.670

ISSN 1948-0210 (online)

ORIGINAL ARTICLE

Basic Study

Mesenchymal stem cells-extracellular vesicles alleviate pulmonary fibrosis by regulating immunomodulators

Ying Gao, Mei-Fang Liu, Yang Li, Xi Liu, Yu-Jie Cao, Qian-Fa Long, Jun Yu, Jian-Ying Li

Specialty type: Cell and tissue engineering

Provenance and peer review: Unsolicited article; Externally peer reviewed.

Peer-review model: Single blind

Peer-review report's classification

Scientific Quality: Grade B, Grade C

Novelty: Grade B

Creativity or Innovation: Grade B

Scientific Significance: Grade B

P-Reviewer: El-Shishtawy MM, Egypt

Received: January 6, 2024

Revised: March 22, 2024

Accepted: May 11, 2024

Published online: June 26, 2024

Processing time: 171 Days and 7.6 Hours

Ying Gao, Department of Respiratory and Critical Care Medicine, Shaanxi Provincial Rehabilitation Hospital, Xi'an 710000, Shaanxi Province, China

Mei-Fang Liu, Department of Respiratory and Critical Care Medicine, Second Affiliated Hospital of Ningxia Medical University (The First People's Hospital of Yinchuan), Yinchuan 750001, Ningxia Hui Autonomous Region, China

Yang Li, School of Clinical Medicine, Xi'an Medical University, Xi'an 710021, Shaanxi Province, China

Xi Liu, Yu-Jie Cao, Jian-Ying Li, Department of Respiratory and Critical Care Medicine, Xi'an Central Hospital, Xi'an 710000, Shaanxi Province, China

Qian-Fa Long, Department of Neurosurgery, Xi'an Central Hospital, Xi'an 710000, Shaanxi Province, China

Jun Yu, Department of Emergency, Xi'an Central Hospital, Xi'an 710000, Shaanxi Province, China

Corresponding author: Jian-Ying Li, MD, Doctor, Department of Respiratory and Critical Care Medicine, Xi'an Central Hospital, No. 163 West Fifth Road, Xi'an 710000, Shaanxi Province, China. l13572168322@163.com

Abstract

BACKGROUND

Pulmonary fibrosis (PF) is a chronic interstitial lung disease characterized by fibroblast proliferation and extracellular matrix formation, causing structural damage and lung failure. Stem cell therapy and mesenchymal stem cells-extracellular vesicles (MSC-EVs) offer new hope for PF treatment.

AIM

To investigate the therapeutic potential of MSC-EVs in alleviating fibrosis, oxidative stress, and immune inflammation in A549 cells and bleomycin (BLM)-induced mouse model.

METHODS

The effect of MSC-EVs on A549 cells was assessed by fibrosis markers [collagen I and α-smooth muscle actin (α-SMA), oxidative stress regulators [nuclear factor E2-related factor 2 (Nrf2) and heme oxygenase-1 (HO-1), and inflammatory regu-

lators [nuclear factor-kappaB (NF-κB) p65, interleukin (IL)-1β, and IL-2]. Similarly, they were assessed in the lungs of mice where PF was induced by BLM after MSC-EV transfection. MSC-EVs ion PF mice were detected by pathological staining and western blot. Single-cell RNA sequencing was performed to investigate the effects of the MSC-EVs on gene expression profiles of macrophages after modeling in mice.

RESULTS

Transforming growth factor (TGF)-β1 enhanced fibrosis in A549 cells, significantly increasing collagen I and α-SMA levels. Notably, treatment with MSC-EVs demonstrated a remarkable alleviation of these effects. Similarly, the expression of oxidative stress regulators, such as Nrf2 and HO-1, along with inflammatory regulators, including NF-κB p65 and IL-1β, were mitigated by MSC-EV treatment. Furthermore, in a parallel manner, MSC-EVs exhibited a downregulatory impact on collagen deposition, oxidative stress injuries, and inflammatory-related cytokines in the lungs of mice with PF. Additionally, the mRNA sequencing results suggested that BLM may induce PF in mice by upregulating pulmonary collagen fiber deposition and triggering an immune inflammatory response. The findings collectively highlight the potential therapeutic efficacy of MSC-EVs in ameliorating fibrotic processes, oxidative stress, and inflammatory responses associated with PF.

CONCLUSION

MSC-EVs could ameliorate fibrosis *in vitro* and *in vivo* by downregulating collagen deposition, oxidative stress, and immune-inflammatory responses.

Key Words: Mesenchymal stem cells; Extracellular vesicles; Pulmonary fibrosis; Oxidative stress response; Epithelial-mesenchymal transition

Core Tip: This study unveils the innovative potential of mesenchymal stem cells-extracellular vesicles (MSC-EVs) in mitigating pulmonary fibrosis (PF). MSC-EVs effectively countered transforming growth factor-β1-induced fibrosis in A549 cells, showcasing a significant reduction in collagen I and α-smooth muscle actin. The treatment exhibited a dual impact, alleviating oxidative stress and inflammatory responses *in vitro*. In PF mouse lungs, MSC-EVs demonstrated remarkable downregulation of fibrotic markers and modulation of oxidative stress and inflammation.

Citation: Gao Y, Liu MF, Li Y, Liu X, Cao YJ, Long QF, Yu J, Li JY. Mesenchymal stem cells-extracellular vesicles alleviate pulmonary fibrosis by regulating immunomodulators. *World J Stem Cells* 2024; 16(6): 670-689
URL: https://www.wjgnet.com/1948-0210/full/v16/i6/670.htm
DOI: https://dx.doi.org/10.4252/wjsc.v16.i6.670

INTRODUCTION

Pulmonary fibrosis (PF) is a chronic and progressive interstitial lung disease of unknown etiology characterized by fibroblast proliferation and extracellular matrix (ECM) formation and accompanied by inflammatory lesions and structural damage[1-4]. PF prevalence is higher among males than females, and most patients are aged > 50 years at diagnosis[5]. Globally, idiopathic PF incidence and prevalence are in the range of 0.09-1.30 and 0.33-4.51 per 10000 persons, respectively[6]. PF is associated with a poor prognosis, with a median survival time of 2-3 years after diagnosis [7]. Chronic alveolar repetitive injury causes the excessive deposition and accumulation of ECM in the lungs[8]. With the continuous deposition of ECM, structural damage, dysfunction, and, eventually, lung failure will appear[8]. Activated fibroblasts are one of the primary sources of myofibroblasts. Transforming growth factor (TGF)-β plays a significant role in promoting the activation, proliferation, and differentiation of epithelial cells and collagen-producing myofibroblasts. Key initiators of fibrosis are epithelial damage, inflammation, epithelial-mesenchymal transformation (EMT), myofibroblast activation, and repetitive cycles of tissue injury[9]. Many patients are often misdiagnosed with heart failure or chronic obstructive pulmonary disease, and the delays in diagnosis prevent early treatment, leading to a median survival rate of 3 years[10-12]. Pirfenidone and nintedanib are the only recommended drugs available for PF treatment, as they both target the fibrotic cascade, leading to a decline in fibroblast and myofibroblast production and ECM accumulation. Still, they generally delay the disease progression[13,14]. Lung transplant and the development of the Lung Allocation Score have increased lung transplantation and survival in recent years, but transplantation remains limited due to a lack of donors[15]. Therefore, it is very necessary to explore alternative treatments for PF.

In recent years, cell therapy based on mesenchymal stromal cells (MSCs) has been widely used to treat various diseases in the lung, liver, and kidney[16]. MSCs are usually obtained from the adult bone marrow, umbilical cord blood, adipose tissue, lung tissue, and placenta[17]. MSCs showed excellent therapeutic effects on tissue injuries, including the lung[18-20], liver[21], heart[22-24], skin[25-27], bone[28], and cartilage[29]. External MSCs are *in vitro* amplified from autologous

or allogeneic sources[30]. External MSCs are known to modulate inflammation and regenerate damaged tissues, thereby remodeling the ECMs, which modulate the apoptosis of stressed cells post-implantation[31]. MSCs from aged human donors exhibit reduced growth rate and capacity and decreased differentiation potential, limiting their applications[32]. Compared with bone marrow-derived MSCs and adipose-derived MSCs, umbilical cord-derived MSCs (UMSCs) have more advantages due to their stronger proliferation and differentiation abilities[33].

The paracrine functions of MSCs can be mediated by extracellular vehicles (EVs)[34]. EVs are released from the endosomal compartment and contain a cargo made of miRNA, mRNA, and proteins from their cells of origin[34]. As EVs are enveloped with a lipid bilayer, the EV-carried cargo is protected from degradation, suggesting that EVs provide advantages for storing and transporting their signaling molecules. Most of these effects may be mediated by their embedded secretome[35].

During the process of PF, epithelial/endothelial cells are damaged in the earlier stage, and inflammatory cytokines are released and initiate a cascade reaction. PF can occur at any age, although it is most prevalent between ages 40 and 70 and is often related to lung aging and oxidative stress[36,37]. The injured alveolar epithelial cells secrete a variety of immune mediators, including cytokines, growth factors, and chemokines, such as TGF-β, interleukin (IL)-1β, IL-2, IL-6, and matrix metalloproteinases, that alter the pulmonary microenvironment and trigger pulmonary inflammatory responses and subsequent fibrous scarring[38].

In this study, the role of MSC-EVs in alleviating PF *in vitro* and *in vivo* was examined. TGF-β1 induced fibrosis in A549 cells, as revealed by collagen I and α-smooth muscle actin (α-SMA) upregulation, but MSC-EV treatment could alleviate it. Oxidative stress regulators [nuclear factor E2-related factor 2 (Nrf2) and heme oxygenase-1 (HO-1)] and inflammatory regulators [nuclear factor-kappaB (NF-κB) p65, and IL-1β] were alleviated by MSC-EVs treatment in A549 cells. MSC-EVs downregulated collagen I and α-SMA, oxidative stress regulators (Nrf2 and HO-1), and inflammatory regulators (NF-κB p65 and IL-1β) in the lungs of PF mice on day 28. In addition, mRNA sequencing of lungs from PF mice revealed upregulation of pulmonary collagen fiber deposition and immune inflammatory response.

MATERIALS AND METHODS

Animal maintenance and ethics statement

The experimental animals selected in this study were adult male C57BL/6 mice, 8-12 wk old, weighing 20 ± 2 g. They were purchased from the Animal Experimentation Centre of the Air Force Military Medical University, China. The experimental animals were bred in a special environment at the Xi'an Central Hospital Center of Science and Education. The indoor temperature was maintained at 25 ± 2 °C. The light/dark cycles, temperature, and humidity were maintained according to experimental standards. The animals had free access to food and water. The feed and bedding were regularly replaced to ensure healthy and stable growth. All animal procedures were performed in accordance with the guidelines for the Care and Use of Laboratory Animals of the National Institutes of Health[39]. All animal procedures were approved by the ethics committee for animal use at Xi'an Central Hospital.

In this study, 90 experimental animals were used. The mice were randomly divided into nine groups, 7-d sham group, 7-d bleomycin (BLM) + phosphate-buffered saline (PBS) group, 7-d BLM + MSC-EVs group, 14-d sham group, 14-d BLM + PBS group, 14-d BLM + MSC-EVs group, 28-d sham group, 28-d BLM + PBS group, and 28-d BLM + MSC-EVs group, with five mice in each group. The *in vivo* model was constructed when the condition of the mice was stable.

MSCs preparation from clinical samples

The donors were healthy, full-term women. The human umbilical cord tissue was from naturally delivered fetuses. For the preparation of allogeneic umbilical cord MSCs, informed consent was obtained from the women before the cells could be collected. Three healthy full-term mothers (27-29 years old) were selected as donors. The procedure conformed to the guidelines of the National Institutes of Health and was approved by the Ethics Committee of Xi'an Central Hospital (No. LW-2023-032).

Preparation of MSC-EVs

Complete media were used, including α-minimum essential media (Gibco, New York, United States) and 16.5% fetal bovine serum (FBS) (Gibco, New York, United States) to amplify MSCs. Surface antigens were detected using primary antibodies against CD105 (BD, United States), CD90 (BD, United States), CD73 (BD, United States), CD45 (BD, United States), and CD34 (BD, United States). The multi-potency of MSCs was tested using the StemPro® osteogenesis, chondrogenesis, and adipogenesis (Gibco, Maryland, United States) differentiation kits according to the manufacturer's instructions[40]. In order to meet the production requirements and culture conditions for obtaining EVs, 3-5 generations of cells were used to collect the supernatant[41]. Exosomes were collected by ultra-centrifugation at 100000 × *g* (XPN-100, Beckman, CA, United States) with conventional FBS for 18 h to prepare exosomal exhausted serum (FBS). The supernatant of upper FBS was collected for subsequent culture. When UMSCs grew to 70% density, they were replaced with a medium with EV-depleted FBS. After 24 h, the supernatant was collected, and the EVs were immediately isolated or frozen at -80 °C[40].

EV separation was performed as we recently reported[42]. The collected supernatants were centrifuged for 300 × *g* for 10 min, 200 × *g* for 10 min, and 10000 × *g* for 30 min (ST16R, Thermo Fisher, United States). The EVs were centrifuged at 100000 × *g* for 70 min (XPN-100, Beckman Coulter, United States) and suspended in sterile PBS at -80 °C. The labeled MSC-EVs were filtered through a 0.22-μm syringe filter immediately before use to avoid staining aggregates[40].

EV protein content was determined by the bicinchoninic acid (BCA) method. Western blotting was performed for CD9 (Abcam, United States) and calnexin (Abcam, United States). The size and morphology distribution of the EVs were assessed using nanoparticle tracking analysis (NS300, Malvern, United Kingdom) and transmission electron microscopy (JEM-1400, JEOL Ltd, Japan), respectively[42].

Culture of A549 cells

The alveolar type II epithelial cells A549 were purchased from the Shanghai Institute of Biochemistry and Cell Biology, Chinese Academy of Sciences (SIBCB, Shanghai, China), and cultured in Dulbecco's Modified Eagle Medium (DMEM) (Gibico; Thermo Fisher Scientific, Inc.) in an incubator containing 5% CO_2 at 37 °C. The medium was changed every 2 d. The cells in the logarithmic growth phase were treated with 0.02% ethylenediamine tetraacetic acid for digestion and collected for subsequent experiments.

Cell counting kit-8 assay

Cell counting kit-8 (CCK-8) kit (C0038, Beyotime, Beijing, China) was used to detect the effects of different concentrations of TGF-β1 on cell proliferation. The A549 cells were inoculated into 96-well plates at a density of 5×10^3 cells/well and divided into five groups with TGF-β1 concentrations of 2.5, 5, 10, 20, and 40 ng/mL, respectively. Cells were detected at 12, 24, 36, and 48 h. After removing the original medium, 10 μL CCK-8 solution was added to each well mixed with 90 μL DMEM and incubated in an incubator for 2 h. The proliferation of the different groups of cells was calculated by measuring the absorbance at the wavelength of 450 nm with a microplate reader.

Establishment of cell model and EV therapy

For the *in vitro* experiment, the cells were divided into four groups: Control group, control + MSC-EVs group, control + TGF-β1 group, and TGF-β1 + MSC-EVs group. In the control group, normal cells were added without any interventions. In the control + MSC-EVs group, MSC-EVs were added to normal cells to verify whether EVs would turn toxic to normal cells. In the control + TGF-β1 group, TGF-β1 was added to the normal cells to induce fibrosis in the cells. In the TGF-β1 + MSC-EVs, MSC-EVs were added to cells having fibrosis to observe the therapeutic effect of MSC-EVs on fibrosis. TGF-β1 induced the fibrosis of A549 cells[43], and the collected cells were plated in 6-well plates at a density of 4×10^5/well. The cells in all groups were starved for 24 h before the original medium was discarded. MSC-EVs and TGF-β1 solution were diluted with DMEM containing 10% FBS. Then, 2 mL diluted TGF-β1 solution was added to the control + TGF-β1 group and was gently shaken and mixed before being placed in an incubator for 24 h. The TGF-β1 + MSC-EVs group was first cultured with the same volume of TGF-β1 as the model group for 24 h, then the original solution was discarded, and 2 mL 10 μg/mL EVs were added for 12 h. The other groups were added with equal volumes of PBS, and the cells in each group were collected after 24 h of culture for subsequent experiments.

Establishment of animal model and EV therapy

Intratracheal BLM induces PF in mice[44]. The mice were randomly divided into the sham group, BLM + PBS group, and BLM + MSC-EVs group. The mice were anesthetized by intraperitoneal injection of 4% chloral hydrate (10 mL /kg). The mice were hung on the operating table of the endotracheal experiment at 60°-70° degrees. The mice were intubated with a 22 G trocar. BLM (5 U /kg) was injected into the trachea of the mice in the BLM + PBS group, and 0.5 mL of air was injected into the trachea with a 1 mL syringe to make the drug enter the lungs. The trocar was pulled out, and the mice were rotated alternately clockwise and counterclockwise to ensure the drug was evenly distributed in both lungs. The mice in the BLM + MSC-EVs treatment group were first injected with BLM in the same way into the trachea. Three hours later, 50 μg of MSC-EVs were injected into the trachea of each mouse again, while PBS of the same concentration was dropped into the trachea of the sham group. The samples were collected at 14 and 28 d. Specimens were used for subsequent experiments.

Hematoxylin and eosin staining and Masson staining

The lung tissue of PF mice was fixed with 4% paraformaldehyde. Paraffin embedding was performed after gradient ethanol dehydration. The specimens were cut into 4-μm-thick sections, dewaxed, stained with hematoxylin for 5 min, processed with alcohol hydrochloride for several seconds, and washed with tap water. Then, the sections were stained with an eosin solution for 5 min. An immunohistochemical (IHC) pen was then used to draw a circle around the tissue to prevent fluid from spilling. Lilchun red was dyed for 8 min, and aniline blue was redyed for 2 min. After washing with anhydrous alcohol three times, neutral gum was added to seal the sections for the microscopic examination.

IHC staining

The fixed specimens were washed, dehydrated, and paraffin-embedded. Citrate buffer pH = 6.0 was added for antigen retrieval. The sections were incubated with 3% hydrogen peroxide for 25 min and washed with PBS thrice. The sections were circled with an IHC pen to prevent the reagent from flowing out. Then, 10% normal goat serum was added to cover the sections evenly, followed by incubation at room temperature for 30 min. The serum was removed, and diluted primary antibody was added and incubated overnight at 4 °C. The sections were rewarmed at room temperature for 30 min and washed with PBS thrice. The diluted secondary antibody was added and incubated at room temperature for 50 min, followed by washing with PBS three times. DAB chromogenic agent was used to cover the sections, followed by hematoxylin for 2 min. Finally, the sections were dehydrated, sealed, and examined under the microscope.

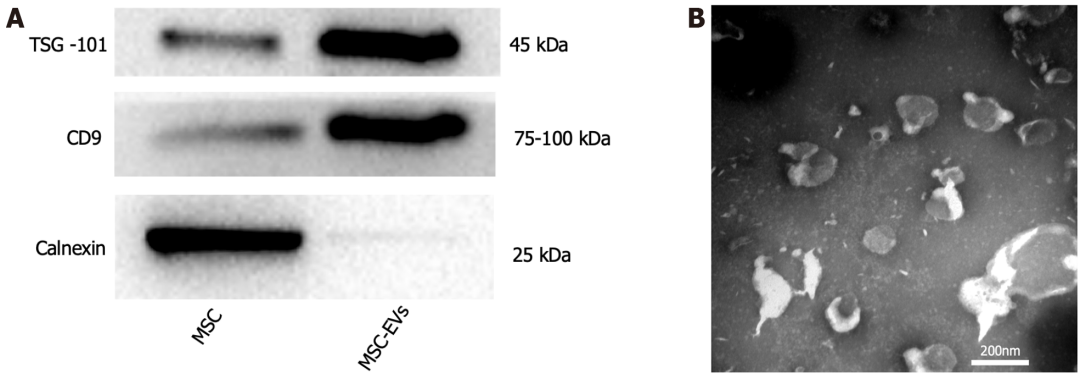

Figure 1 Extraction and identification of mesenchymal stem cells-extracellular vesicles. A: Expression of mesenchymal stem cell (MSC) and MSC-extracellular vesicles (EVs) related proteins (calnexin is the signature protein of MSC, CD9, and TSG101 are the signature proteins of MSC-EVs. The expression level of calnexin in MSC is more obvious than that in MSC-EVs, while the expression level of TSG-101 and CD9 in MSC-EVs is more obvious than that in MSC; B: Morphology of MSC-EVs under electron microscope. MSC: Mesenchymal stem cell; EV: Extracellular vesicle.

mRNA sequencing

Combined with previous pathological staining results, four mice in the sham and BLM + PBS groups were sacrificed 28 d after administration to remove lung tissue. The lung specimens were immersed in a 1.5 mL enzyme-free centrifuge tube containing RNA Wait (Solarbio, SR0020, Beijing, China). Then, it was refrigerated at 4 °C for 24 h and stored at -80 °C. Total RNA was extracted from the tissue samples by RNAiso Plus Total RNA extraction reagent (Cat#9109, TAKARA) according to the manufacturer's procedures, and it was subjected to electrophoresis for quality inspection and purification. The purified total RNA was separated and segmented. The first and second strand cDNA were synthesized, modified, and enriched for inspection again. According to the Illumina user operation manual, the flow cell carrying the cluster was checked on the computer, and the pair-end program was selected to carry out double-end sequencing and analyze real-time data. Finally, edgeR was used to analyze the differentially expressed genes between samples, and the difference multiple (fold change) > 2 and $P < 0.05$ were used as the criteria to screen the differentially expressed mRNAs.

Western blot analysis

Total proteins extracted from cells and tissues using RIPA buffer (Beyotime, Shanghai, China) were quantified using a BCA detection kit (Beyotime, Shanghai, China). The isolated proteins were electrically transferred to a polyvinylidene fluoride membrane by 10% sodium dodecyl sulfate-polyacrylamide gel electrophoresis (Beyotime, Shanghai, China). The membrane was sealed with 5% skim milk for 2 h. After the sealing, the membranes were washed thrice with PBS, 10 min each time. Rabbit anti-α-SMA (Proteintech, 14395-1-AP 1:6000), rabbit anti-collagen I (Abcam, AB260043, 1:1000), rabbit anti-NRF2 (Invitrogen, PA5-27882, 1:1000), rabbit anti-HO-1 (Proteintech, 10701-1-AP 1:3000), mouse anti-NF-κB p65 (Cell Signaling Technology, 6956S, 1:1000), rabbit anti-IL-2 (Cell Signaling Technology, 12239, 1:1000), rabbit anti-IL-1β (Cell Signaling Technology, 31202, 1:1000), rabbit anti-β-actin (ABclonal, AC026, 1:100000), rabbit anti-CD9 (Abcam, AB92726, 1:2000), and rabbit anti-TSG101 (Abcam, AB125011, 1:2000) were used to soak the membranes, followed by overnight incubation in a dark environment at 4 °C. The next day, the membranes were removed, rewarmed at room temperature for 1 h, and washed three times with PBS for 10 min each. Goat anti-mouse antibody (Thermo, 1:50000) with horseradish peroxidase combined with immunoglobulin G and goat anti-rabbit antibody (Thermo, 1:25000) were incubated for 2 h and immunized with enhanced chemiluminescence (Millipore, BB-3501, Ameshame, United Kingdom). The protein bands were imaged and analyzed using the Bio-Rad imaging system (California, United States).

Statistical analysis

All data were analyzed using SPSS 26.0 (IBM, Armonk, NY, United States). Image-pro Plus was used to perform statistical analysis on the lesion area size of the pathological sections. The graphs were plotted using GraphPad Prism 8. The data were expressed as means ± SD. One-way analysis of variance (ANOVA) was used to compare multiple groups, and the independent sample *t*-test was used to compare two groups. $P < 0.05$ indicated statistically significant differences.

RESULTS

Extraction and identification of MSC-EVs

MSC culture, extraction, and identification of MSC-EVs were performed. Vesicle-like material ranging from 40-200 nm in diameter was observed by transmission electron microscopy. The expression levels of CD9, TSG101, and calnexin in the MSC and MSC-EVs groups were detected by western blot. The results showed that the CD9 and TSG101 expression levels were significantly higher in the MSC-EVs group than in the MSC group, as they are typical EV surface markers, and the expression level of calnexin in the MSC group was higher than in the MSC-EVs group (Figure 1A and B). These results confirmed that the EVs derived from umbilical cord MSCs were purified in accordance with the standard to be used for

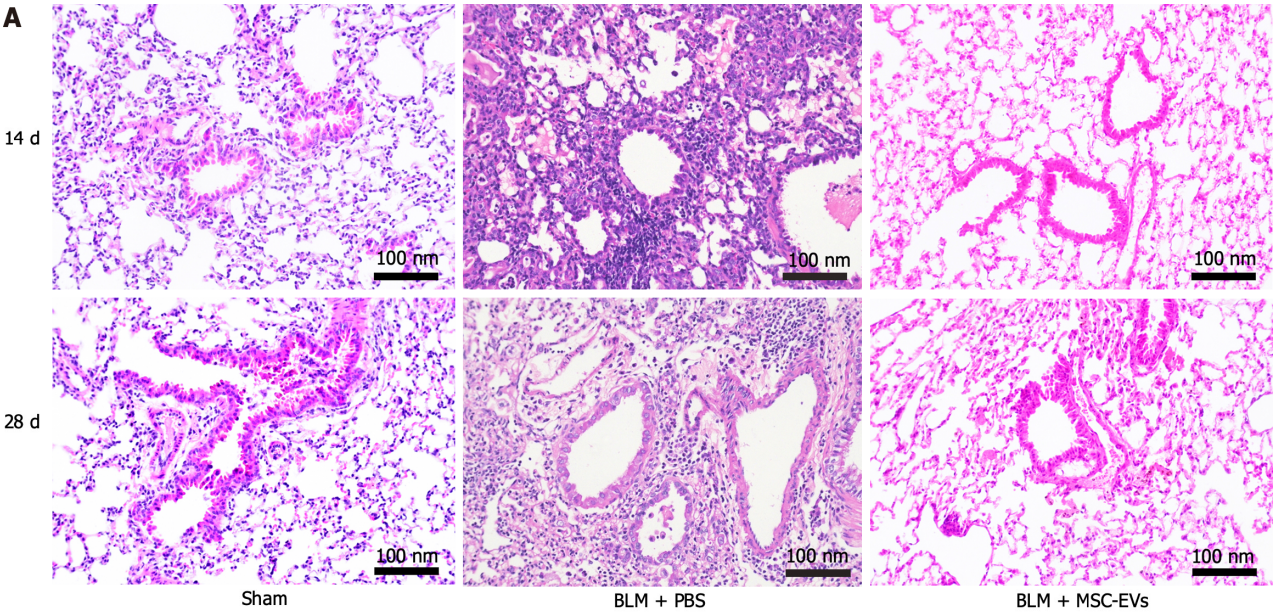
A
14 d
28 d
100 nm
Sham
BLM + PBS
BLM + MSC-EVs

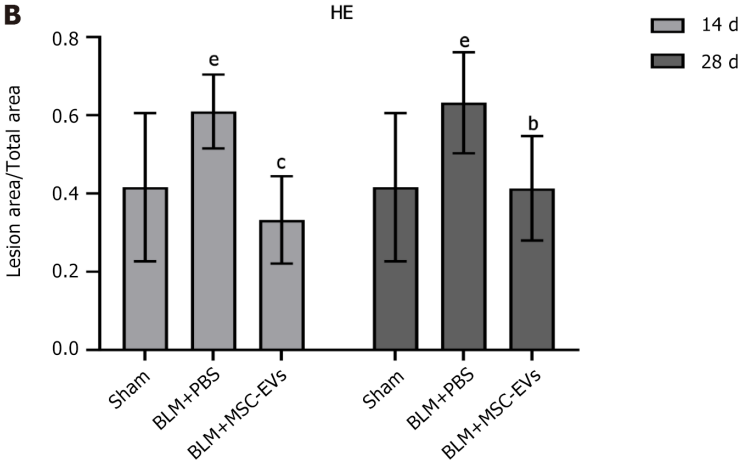
B
HE
14 d
28 d
Lesion area/Total area
0.8
0.6
0.4
0.2
0.0
e
e
c
b
Sham
BLM+PBS
BLM+MSC-EVs
Sham
BLM+PBS
BLM+MSC-EVs

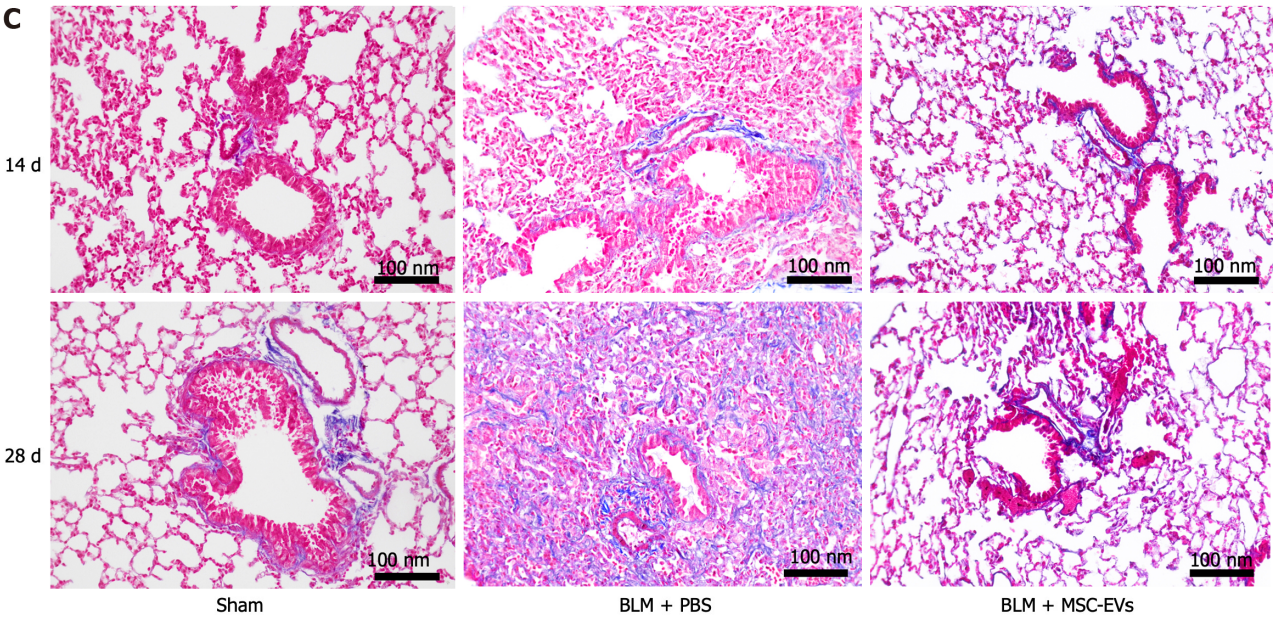
C
14 d
28 d
100 nm
Sham
BLM + PBS
BLM + MSC-EVs

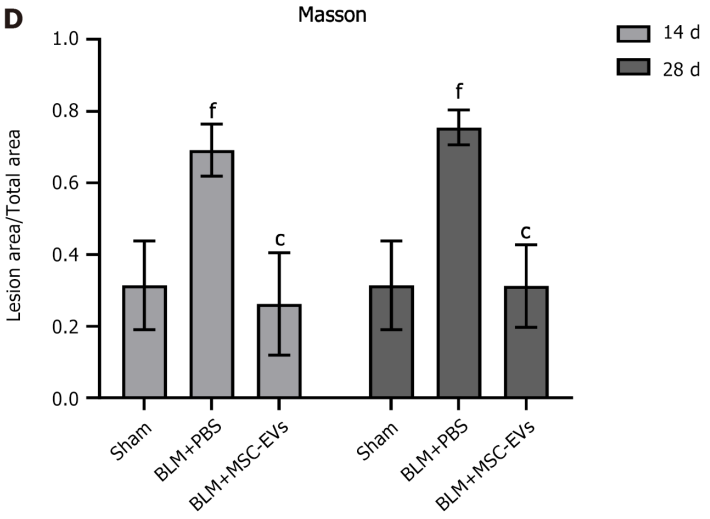

Figure 2 Bleomycin can induce pulmonary fibrosis and inflammatory infiltration in mice. A: Hematoxylin and eosin (HE) staining of lung tissue of mice in each group on days 14 and 28 after administration. Inflammatory cells are basophilic (blue-purple granules), and their number represents the severity of inflammation in the lung tissue of mice; B: The quantitative statistical analysis of HE staining on days 14 and 28 among the three groups. The ordinate represents the percentage of the inflammatory area in the total area, and the abscissa represents the grouping. In the bleomycin group, there were significant inflammatory reactions on day 14 ($^eP < 0.01$ *vs* sham group) and day 28 ($^eP < 0.01$ *vs* sham group). After exosome treatment, the inflammatory reactions were significantly improved on day 14 ($^cP < 0.001$) and day 28 ($^bP < 0.01$); C: Masson staining of lung tissue of mice in each group on days 14 and 28 after administration. Collagen fibers appear blue, and their number represents the severity of collagen deposition in the lungs of mice; D: The quantitative statistical analysis of Masson staining. The ordinate represents the percentage of collagen fiber deposition area in the total area, and the abscissa represents the grouping. In the bleomycin group, significant collagen deposition occurred on day 14 ($^fP < 0.001$ *vs* sham group) and day 28 ($^fP < 0.001$ *vs* sham group). After exosome treatment, the collagen deposition decreased on day 14 ($^cP < 0.001$) and day 28 ($^cP < 0.001$). MSC: Mesenchymal stem cell; EV: Extracellular vesicle; BLM: Bleomycin; PBS: Phosphate buffered saline.

further experimental studies.

BLM can induce PF and inflammatory infiltration in mice

The lung tissues of BLM-treated mice in each group were stained with hematoxylin and eosin and Masson staining. In the sham group, there were no obvious inflammatory cell infiltration and collagen deposition in the lung tissue of mice, the alveolar structure was clear and intact, and there were no obvious congestion, edema, or widening of alveolar septa (Figure 2A and B). In the BLM + PBS group, inflammatory cell infiltration (Figure 2A and B) and collagen fiber deposition (Figure 2C and D) were significantly higher in the lung tissue compared to other groups, collapsed alveolar structure, and dilated capillaries were observed around the alveoli, with widening of the alveolar septa. However, significant structural changes were observed in the lungs after intratracheal infusion of MSC-EVs. Compared with the sham group, the degree of inflammatory injury and collagen deposition in the lung tissue of mice in the BLM + PBS group were significantly increased after 14 and 28 d. After the infusion of MSC-EVs, a significant decline in the lesions was observed ($P < 0.05$) (Figure 2B and D).

The pathogenesis of PF may involve collagen deposition, oxidative stress, and immunoinflammatory response

According to the previous pathological staining results, the inflammatory infiltration and collagen deposition in the lungs of mice were more obvious 28 d after administration. Therefore, lung tissues of mice in the sham group and BLM + PBS group 28 d after administration were used for mRNA sequencing to screen for related differentially expressed genes.

Screening was based on the absolute fold change value of ≥ 2 and $P < 0.05$. A total of 133 upregulated genes and 124 downregulated genes were screened (Figure 3A-C). The screening results showed that a differential expression mainly occurred in genes involved in collagen deposition, microfiber-associated protein, and immunoglobulin structure, including nuclear factor receptor subfamily and other related genes. Therefore, the development of PF in C57BL/6 mice may be related to oxidative stress and the activation of immune pathways, leading to collagen deposition in lung tissue.

Assessing the optimal concentration and time of fibrosis in A549 cells

The optimum concentration and time of TGF-β1 in A549 cells were screened by the CCK8 method. The larger the OD value, the higher the number of viable cells. Simultaneously, the higher the slope between adjacent gradient concentrations, the higher the number of proliferating cells at that concentration. The optimal concentration of TGF-β1 was finally screened as 10 ng/mL, and the optimal culture time was 48 h (Figure 4).

MSC-EVs may alleviate PF by inhibiting EMT

The influence of TGF-β1 on the expressions of collagen I and α-SMA related molecules on A549 cells was verified by western blot. TGF-β1 could promote fibrosis in A549 cells, and the expression levels of collagen I and α-SMA were significantly increased compared with those of the control group ($P < 0.05$). After MSC-EVs treatment, the fibrosis

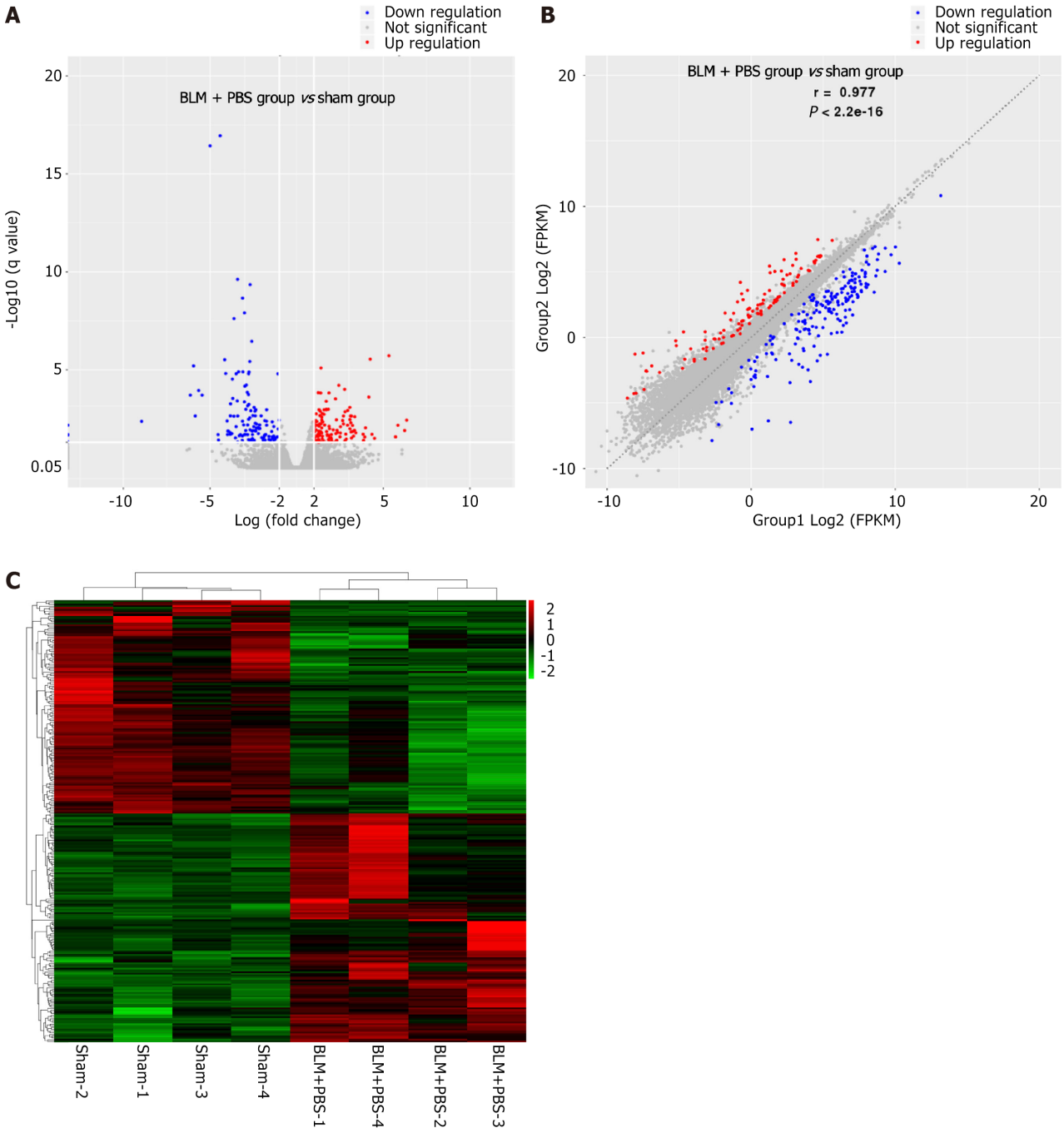

Figure 3 The pathogenesis of pulmonary fibrosis may be related to collagen deposition, oxidative stress, and immunoinflammatory response. A: Volcano map of differentially expressed genes between sham group and bleomycin (BLM) + PBS group; B: Scatter plot of differentially expressed genes between the sham and BLM + PBS groups; C: Heat map of differentially expressed genes between the sham and BLM + PBS groups. BLM: Bleomycin; PBS: Phosphate buffered saline.

induced by TGF-β1 was significantly reduced ($P < 0.05$). However, the addition of MSC-EVs in normal A549 cells did not alter collagen I and α-SMA levels compared with controls ($P > 0.05$) (Figure 5A-C). Meanwhile, IHC staining was used to verify the expression of the above proteins in the lung tissue of mice in the *in vivo* model. TGF-β1 expression in the lung tissue of mice treated with BLM + PBS was significantly higher than in the sham-treated mice ($P < 0.05$), and collagen I and α-SMA expression was significantly increased in the lung tissue of mice ($P < 0.05$). After MSC-EVs treatment, the expression of TGF-β1, collagen I, and α-SMA was decreased compared with the BLM + PBS group ($P < 0.05$) (Figure 5D-I). Similarly, western blot results from the *in vivo* experiments were consistent with the IHC results ($P < 0.05$) (Figure 5J-L). Therefore, TGF-β1 can induce fibrosis of alveolar epithelial cells, BLM can induce EMT in mouse lung tissue, MSC-EVs may alleviate PF by regulating this mechanism, and MSC-EVs do not cause fibrosis in normal cells.

MSC-EVs may alleviate PF in mice by regulating oxidative stress response in lung tissue

Nrf2 and HO-1 are key molecules involved in regulating oxidative stress, and they were verified by western blot. Under

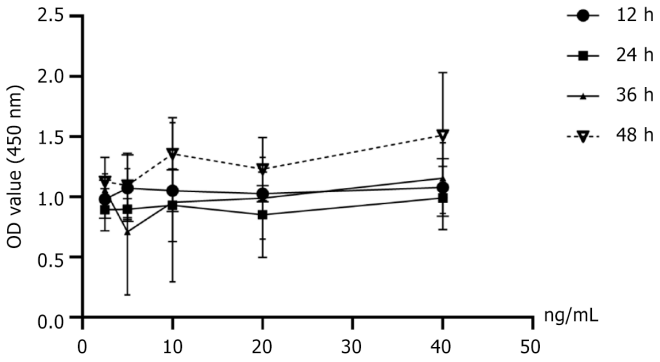

Figure 4 The optimum concentration and time were screened using the cell counting kit-8 method.

certain circumstances, TGF-β1 could induce oxidative stress in A549 cells, and Nrf2 and HO-1 expression levels significantly increased after TGF-β1 addition ($P < 0.05$). Their expression levels were significantly downregulated after MSC-EV treatment ($P < 0.05$). MSC-EVs did not upregulate the expression of oxidative stress-related molecules in normal cells ($P > 0.05$) (Figure 6A-C). Meanwhile, IHC staining was used to verify *in vivo* the results obtained *in vitro*. Nrf2 and HO-1 expression in the lung tissue of the mice in the BLM + PBS group was significantly higher than in the sham group ($P < 0.05$). After treatment with MSC-EVs, the expression of Nrf2 in the BLM + MSC-EVs group did not change significantly at 14 d after administration ($P > 0.05$), but there was a significant shift on day 28 ($P < 0.05$). In addition, Nrf2 downstream molecule HO-1 expression in the BLM + PBS group was significantly higher than in the sham group at 14 and 28 d after administration. In comparison, the HO-1 expression in the MSC-EVs group was significantly lower at 14 and 28 d ($P < 0.05$) (Figure 6D-G). Similarly, western blot results of lung tissue of mice in each group showed that the changes in Nrf2 in the BLM + PBS and BLM + MSC-EVs group on days 7 and 14 ($P < 0.05$) were the same as those in the IHC group on day 14. The changes at 28 d after administration were consistent with IHC staining ($P < 0.05$). Secondly, the expression of HO-1 in the lung tissues of the mice in each group was also consistent with the change in IHC staining ($P < 0.05$) (Figure 6H-J). Our findings indicated that MSC-EVs did not induce oxidative stress in normal cells but could rapidly regulate the oxidative stress response after oxidative stress in cells to improve oxidative damage and further alleviate PF. In addition, other mechanisms may regulate the oxidative stress response between Nrf2 and HO-1 in PF.

MSC-EVs can inhibit the inflammatory response in the process of PF

NF-κB p65, IL-1β, and IL-2 play key regulatory roles in various immune-inflammatory diseases and were detected in A549 cells by western blot. TGF-β1 induced fibrosis in A549 cells produced an inflammatory reaction at the same time. NF-κB p65 and IL-1β expression levels were significantly increased after TGF-β1 addition, and they were significantly downregulated after MSC-EV treatment ($P < 0.05$). Still, there were no significant changes when MSC-EVs were administered to normal cells ($P > 0.05$) (Figure 7A-C). Meanwhile, IHC staining was used to verify *in vivo* the results obtained *in vitro*. The expression of inflammation-related proteins (NF-κB p65, IL-1β, and IL-2) in lung tissues of mice treated with BLM + PBS was significantly higher than in sham-treated mice ($P < 0.05$). After MSC-EV treatment, NF-κB p65, IL-1β, and IL-2 expression levels were significantly decreased compared with the BLM + PBS group ($P < 0.05$) (Figure 7F-I). The western blot results were consistent with the IHC results ($P < 0.05$) (Figure 7D and E). These results indicated that the development of PF may be accompanied by acute and chronic inflammatory reactions in lung tissue, which may further cause lung tissue injury, leading to PF. MSC-EVs could not change the physiological state of normal cells, but they could improve the immune inflammatory response in the process of cell fibrosis. MSC-EVs can alleviate lung tissue injury by inhibiting lung tissue fibrosis accompanied by an immune inflammatory response, downregulating the PF process.

DISCUSSION

PF is a chronic progressive disease with high incidence and poor prognosis. Several factors contribute to PF, including exposure to toxins, tobacco smoke, medical conditions, radiation therapy, viral infections, and some drugs[45,46]. Damage and abnormal repair of the lung interstitium leads to the formation of scar tissue that is different from the structure and function of the normal lung interstitium[4]. In the process of PF, epithelial/endothelial cells are damaged, releasing inflammatory cytokines, further triggering a cascade of reactions[9]. Loss of antifibrotic properties of intact epithelial cells and increased secretion of pro-fibrotic factors from damaged epithelial cells may lead to fibrosis[47]. At present, the treatment of PF is limited and has many adverse reactions that greatly limit the application of drugs. It is difficult to perform lung transplantation in respiratory diseases because of the small number of donors. Therefore, finding new therapeutic strategies for PF is highly important. In this study, the role of MSC-EVs in alleviating PF *in vivo* and *in vitro* was examined. MSC-EV treatment could alleviate TGF-β1-induced fibrosis in A549 cells, which was confirmed by the downregulation of collagen I and α-SMA, oxidative stress regulators (Nrf2 and HO-1) and inflammatory regulators (NF-κB p65 and IL-1β). Like the PF mice model, MSC-EVs infusion into the lungs could downregulate collagen I and α-SMA, oxidative stress regulators (Nrf2 and HO-1), and inflammatory regulators (NF-κB p65 and IL-1β). Upregulation of

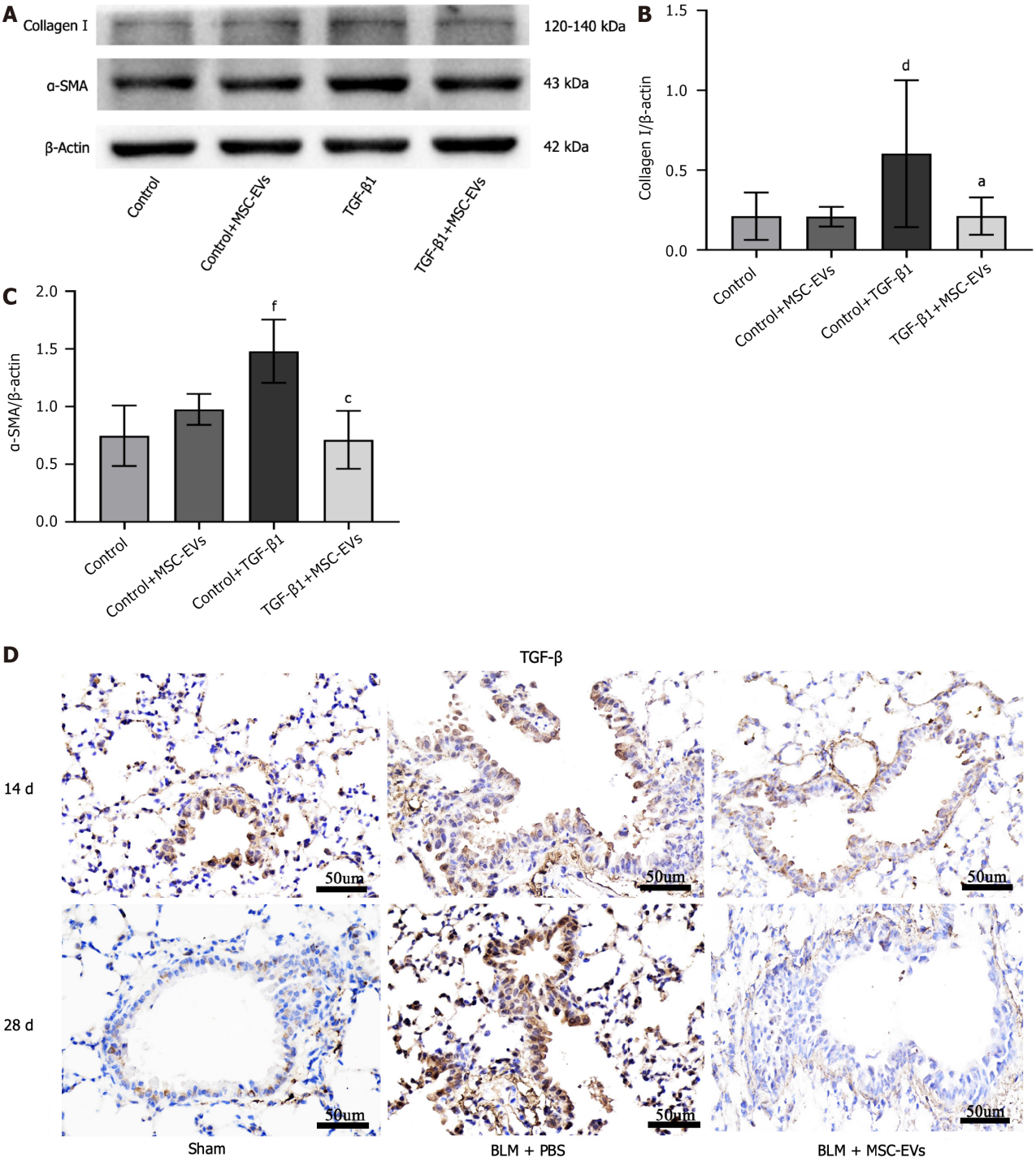
A
Collagen I
α-SMA
β-Actin
120-140 kDa
43 kDa
42 kDa
Control
Control+MSC-EVs
TGF-β1
TGF-β1+MSC-EVs
B
Collagen I/β-actin
C
α-SMA/β-actin
D
TGF-β
14 d
28 d
50um
Sham
BLM + PBS
BLM + MSC-EVs
E
TGF-β
14 d
28 d
Lesion area/Total area
Sham
BLM+PBS
BLM+MSC-EVs

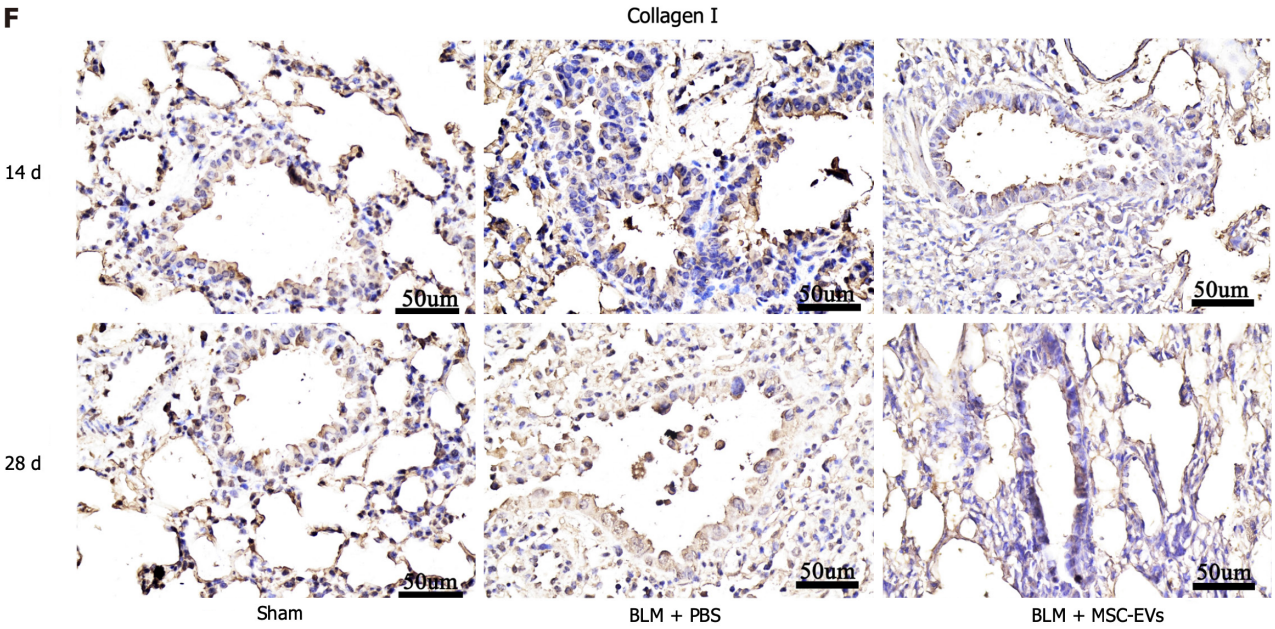
F
Collagen I
14 d
28 d
50um
Sham
BLM + PBS
BLM + MSC-EVs

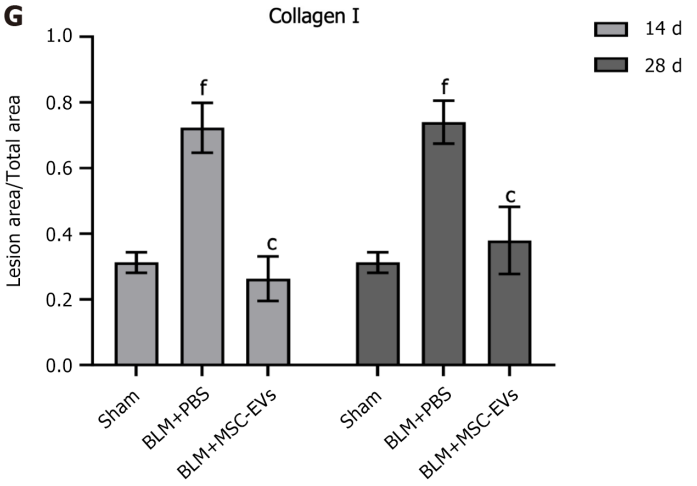
G
Collagen I
14 d
28 d
Lesion area/Total area
1.0
0.8
0.6
0.4
0.2
0.0
f
c
Sham
BLM+PBS
BLM+MSC-EVs

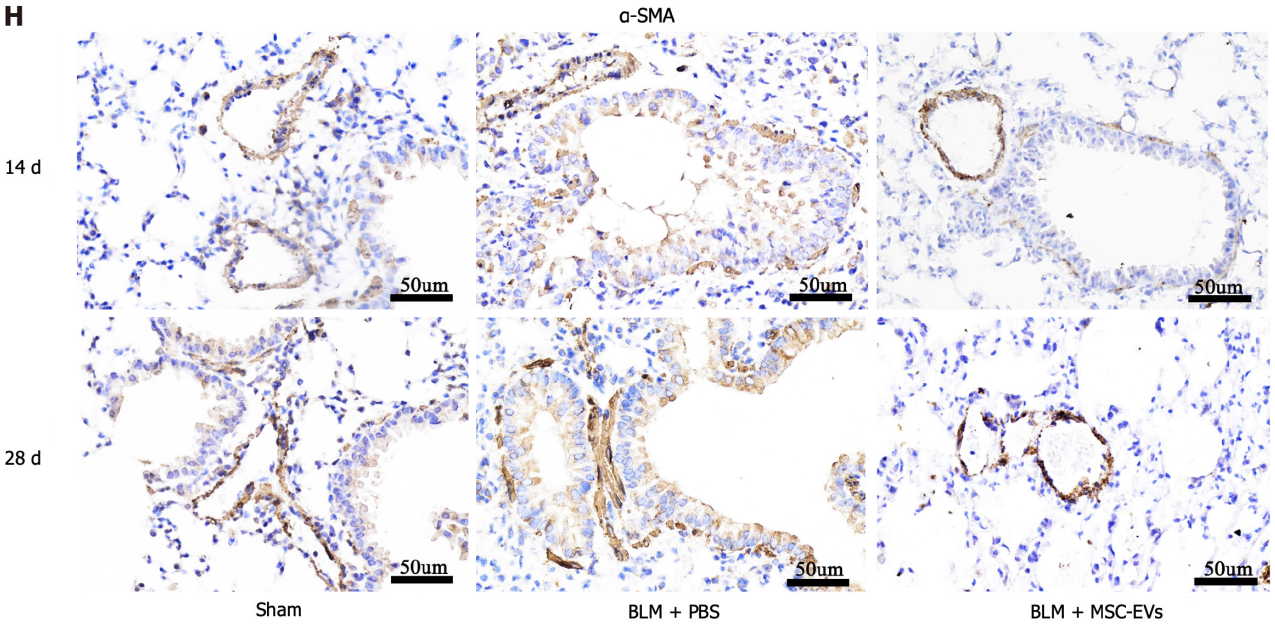
H
α-SMA
14 d
28 d
50um
Sham
BLM + PBS
BLM + MSC-EVs

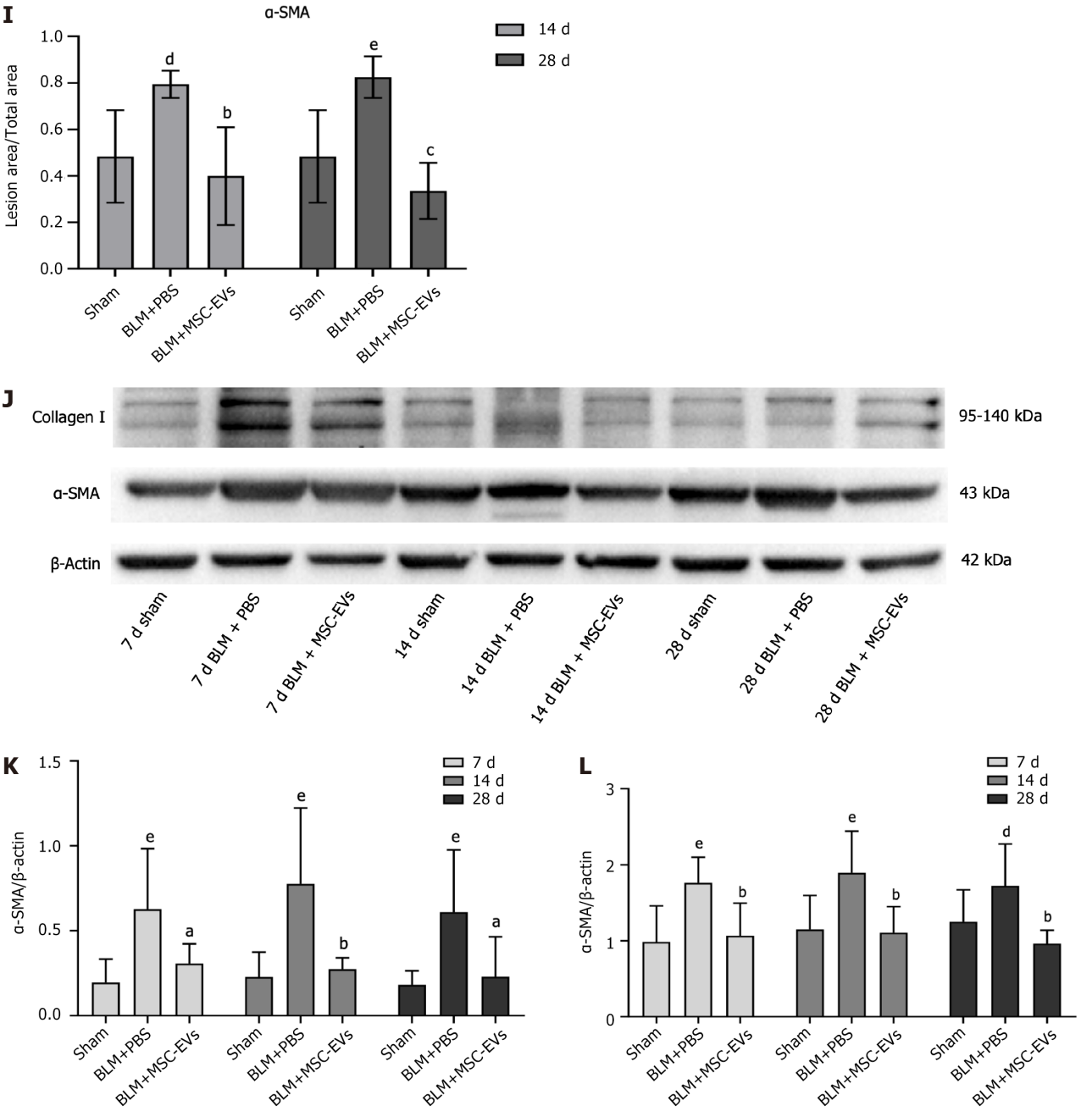

Figure 5 Mesenchymal stem cells-extracellular vesicles may alleviate pulmonary fibrosis by inhibiting epithelial-mesenchymal transformation. A: The expressions of collagen I and α-smooth muscle actin (α-SMA) in A549 cells of each group were verified by western blot; B and C: The statistical analysis of the expression levels of each protein. Mesenchymal stem cells-extracellular vesicles (MSC-EVs) did not affect normal cell proliferation and differentiation ($P > 0.05$). Transforming growth factor (TGF)-β can induce epithelial-mesenchymal transformation of cells (collagen I: $^{d}P < 0.05$ *vs* control group; α-SMA: $^{f}P < 0.001$ *vs* control group). However, MSC-EVs can reverse the epithelial-mesenchymal transformation process caused by TGF-β (collagen I: $^{a}P < 0.05$; α-SMA: $^{c}P < 0.001$); D-I: The expression of TGF-β1, collagen I, and α-SMA in lung tissue was observed by immunohistochemical (IHC) staining (D, F, and H). The statistical analysis of the expression level of TGF-β, collagen I, and α-SMA in IHC staining (E, G, and I). On day 14 and day 28, TGF-β1 (14 d: $^{f}P < 0.001$ *vs* sham group; 28 d: $^{f}P < 0.001$ *vs* sham group), collagen I (14 d: $^{f}P < 0.001$ *vs* sham group; 28 d: $^{f}P < 0.001$ *vs* sham group) and α-SMA (14 d: $^{d}P < 0.05$ *vs* sham group; 28 d: $^{e}P < 0.01$ *vs* sham group) deposition were observed in the bleomycin + phosphate buffered saline group, and the above pathological changes could be reversed after MSC-EVs treatment [TGF-β1 (14 d: $^{c}P < 0.001$; 28 d: $^{c}P < 0.001$)], collagen I (14 d: $^{c}P < 0.001$; 28 d: $^{c}P < 0.001$) and α-SMA (14 d: $^{b}P < 0.01$; 28 d: $^{c}P < 0.001$); J: The western blot results of each protein's expression in mice's lung tissue in each group; K and L: The statistical analysis of western blot results of each protein in mouse lung tissue. No matter whether on day 7, 14, or 28, the expression of epithelial-mesenchymal transformation gene-related collagen I (7 d: $^{e}P < 0.01$ *vs* sham group; 14 d: $^{e}P < 0.01$ *vs* sham group; 28 d: $^{e}P < 0.01$ *vs* sham group) and α-SMA (7 d: $^{e}P < 0.01$ *vs* sham group; 14 d: $^{e}P < 0.01$ *vs* sham group; 28 d: $^{d}P < 0.05$ *vs* sham group) in lung tissue of mice was significantly higher than that in the sham group. After MSC-EVs treatment, the expression of collagen I and α-SMA decreased significantly at 7 d (collagen I: $^{a}P < 0.05$; α-SMA: $^{b}P < 0.01$) in the acute phase, 14 d in the subacute phase (collagen I: $^{b}P < 0.01$; α-SMA: $^{b}P < 0.01$) and 28 d in chronic phase (collagen I: $^{a}P < 0.05$; α-SMA: $^{b}P < 0.01$). These results indicate that the development of pulmonary fibrosis is long-term, and the anti-epithelial mesenchymal transformation of MSC-EVs is stable and long-lasting. MSC: Mesenchymal stem cell; EV: Extracellular vesicle; BLM: Bleomycin; PBS: Phosphate buffered saline; TGF: Transforming growth factor; α-SMA: Alpha smooth muscle actin.

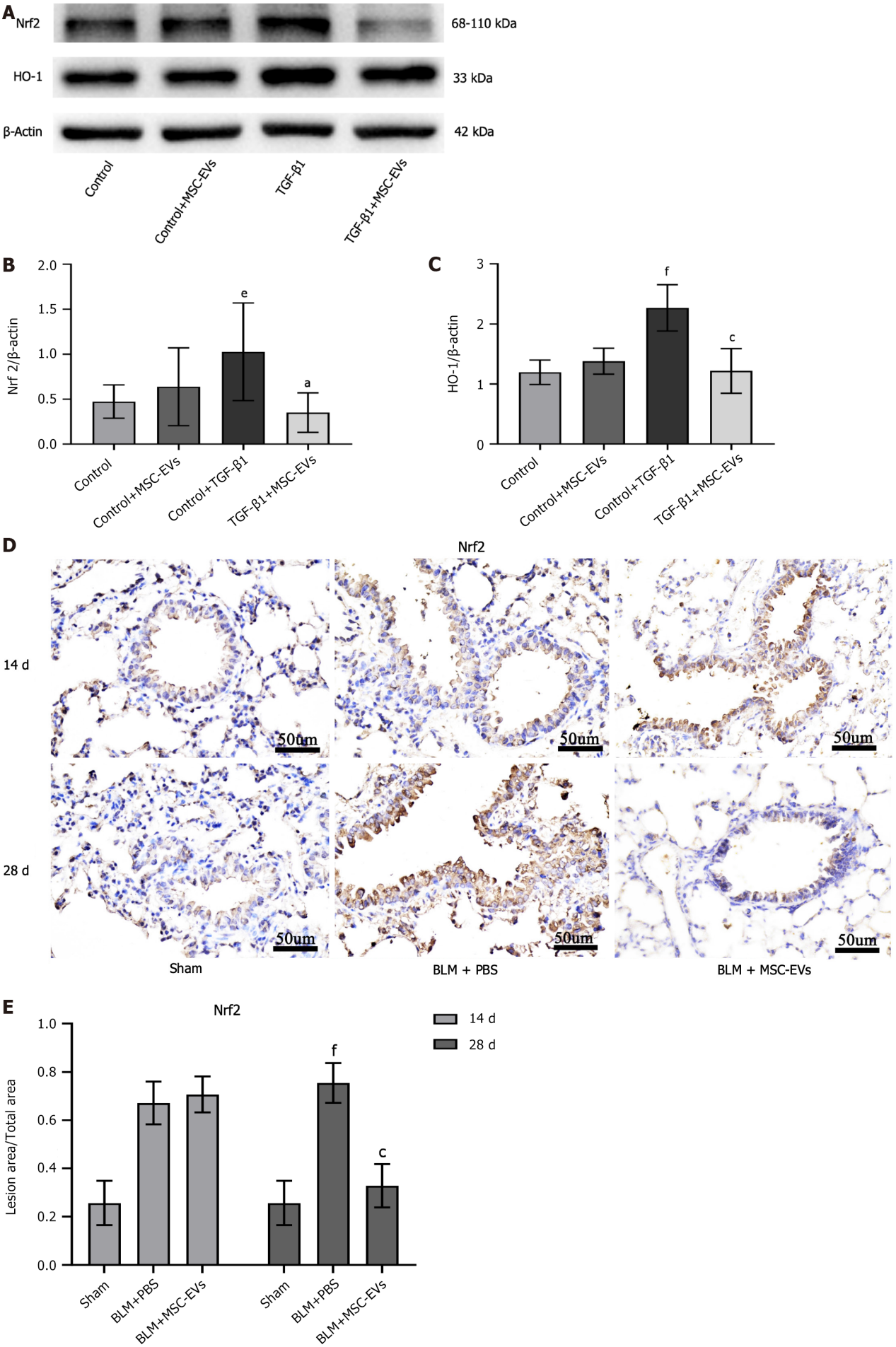
A
Nrf2
HO-1
β-Actin
68-110 kDa
33 kDa
42 kDa
Control
Control+MSC-EVs
TGF-β1
TGF-β1+MSC-EVs
B
Nrf 2/β-actin
2.0
1.5
1.0
0.5
0.0
e
a
Control
Control+MSC-EVs
Control+TGF-β1
TGF-β1+MSC-EVs
C
HO-1/β-actin
3
2
1
0
f
c
Control
Control+MSC-EVs
Control+TGF-β1
TGF-β1+MSC-EVs
D
Nrf2
14 d
28 d
50um
Sham
BLM + PBS
BLM + MSC-EVs
E
Nrf2
Lesion area/Total area
1.0
0.8
0.6
0.4
0.2
0.0
14 d
28 d
f
c
Sham
BLM+PBS
BLM+MSC-EVs
Sham
BLM+PBS
BLM+MSC-EVs

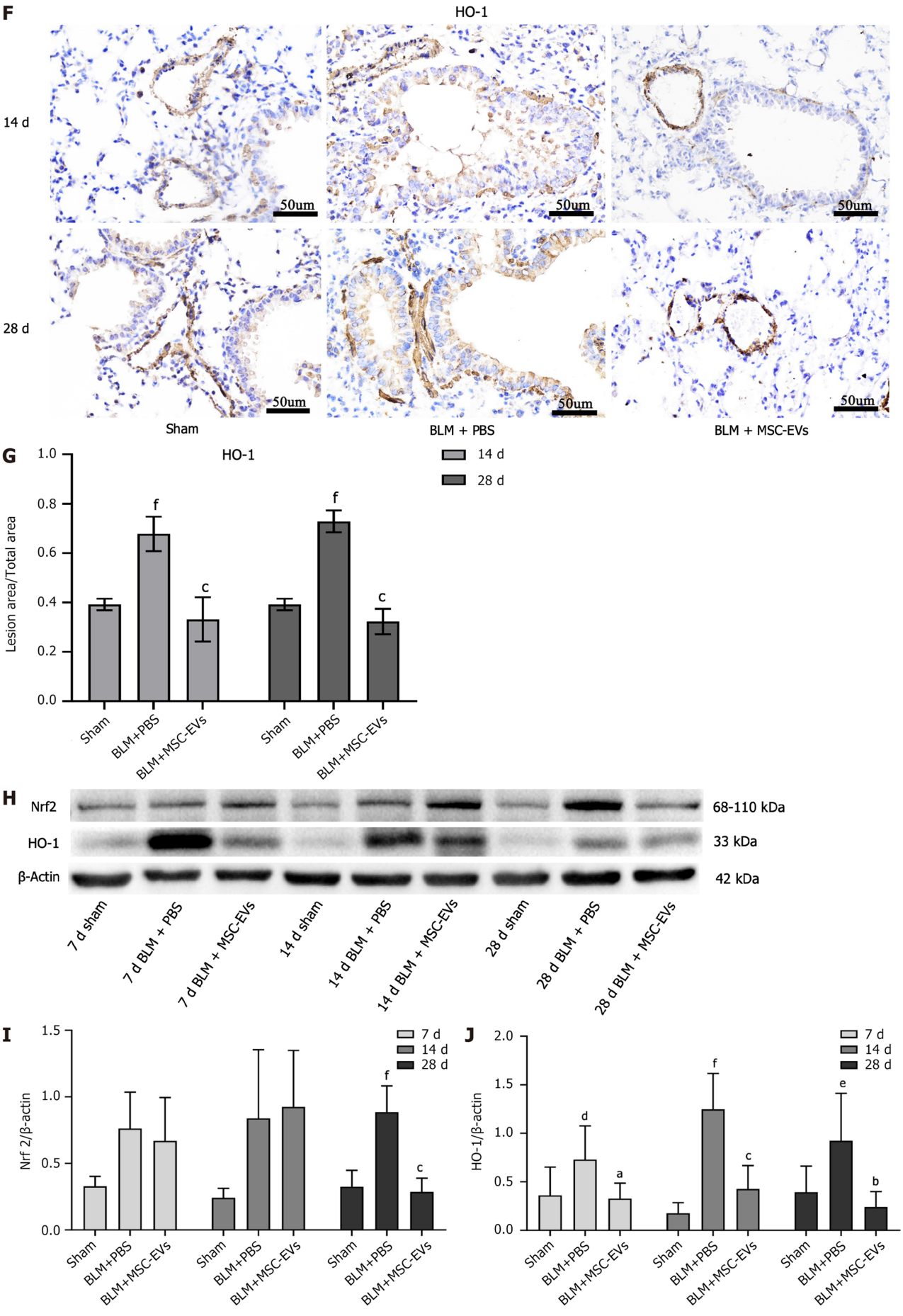

Figure 6 Mesenchymal stem cells-extracellular vesicles may alleviate pulmonary fibrosis in mice by regulating oxidative stress response

in lung tissue. A: The expressions of nuclear factor E2-related factor 2 (Nrf2) and heme oxygenase-1 (HO-1) in A549 cells of each group were verified by western blot; B and C: The statistical analysis of the expression levels of each protein. Mesenchymal stem cells-extracellular vesicles (MSC-EVs) can't cause oxidative stress in cells ($P > 0.05$), and transforming growth factor (TGF)-β can cause obvious oxidative stress in A549 (Nrf2: $^{e}P < 0.01$ *vs* control group; HO-1: $^{f}P < 0.001$ *vs* control group), while MSC-EVs can reverse the above pathological process brought about by TGF-β (Nrf2: $^{a}P < 0.05$; HO-1: $^{c}P < 0.001$); D-G: The expression of Nrf2 and HO-1 in lung tissue was observed by immunohistochemical (IHC) staining (D and F). The statistical analysis of the expression level of each protein in IHC staining (E and G). On day 14 and day 28, Nrf2 (14 d: $P > 0.05$; 28 d: $^{f}P < 0.001$ *vs* sham group), HO-1 (14 d: $^{f}P < 0.001$ *vs* sham group; 28 d: $^{f}P < 0.001$ *vs* sham group) deposition was observed in the bleomycin + phosphate buffered saline group, and the above pathological changes could be reversed after MSC-EVs treatment [Nrf2 (14 d: $P > 0.05$; 28 d: $^{c}P < 0.001$), HO-1 (14 d: $^{c}P < 0.001$; 28 d: $^{c}P < 0.001$)]; H: The western blot results of the expression of Nrf2 and HO-1 in lung tissue of mice in each group; I and J: The statistical analysis of western blot results of each protein in mouse lung tissue. There were no significant changes in Nrf2 expression on day 7 ($P > 0.05$) and day 14 ($P > 0.05$) of pulmonary fibrosis development, but an increase in Nrf2 expression could be detected on day 28 ($^{f}P < 0.001$ *vs* sham group). No matter whether on day 7, 14, or 28, the expression of HO-1 (7 d: $^{d}P < 0.05$ *vs* sham group; 14 d: $^{f}P < 0.001$ *vs* sham group; 28 d: $^{e}P < 0.01$ *vs* sham group) in lung tissue of mice was significantly higher than that in the sham group. After MSC-EVs treatment, the expression of HO-1 decreased significantly at 7 d ($^{a}P < 0.05$) in the acute phase, 14 d in the subacute phase ($^{c}P < 0.001$), and 28 d in the chronic phase ($^{b}P < 0.01$). However, the expression of Nrf2 decreased significantly only on day 28 ($^{c}P < 0.001$). MSC: Mesenchymal stem cell; EV: Extracellular vesicle; BLM: Bleomycin; PBS: Phosphate buffered saline; Nrf2: Nuclear factor E2-related factor 2; HO-1: Heme oxygenase-1.

pulmonary collagen fiber deposition and immune inflammatory response were observed from the lungs of PF mice through mRNA sequencing.

EMT has been a research hotspot in PF in recent years. Among the many molecules that cause EMT, TGF-β is considered a key molecule that induces EMT in lung tissues during the process of PF[48]. In the present study, immunohistochemical staining of the lung tissue of C56BL/6 mice revealed that BLM could upregulate TGF-β expression in the lung tissue of mice, leading to EMT. After MSC-EVs treatment, TGF-β1 levels were downregulated in lung tissue, and EMT was relieved. The downregulation of collagen I and α-SMA confirmed the results, revealing the reduction in collagen deposition in the lung. Therefore, it was concluded that BLM-induced PF in mice caused collagen deposition in the lung, and MSC-EV treatment could significantly alleviate the above pathological changes.

Oxidative stress is caused by the imbalance between oxidants and antioxidants, which is related to the pathophysiological characteristics of PF[49]. Nrf2, also known as nuclear transcription factor E2-related factor 2, is a key molecule in regulating oxidative stress. Under oxidative stress, Nrf2 inhibitor Kelch-like erythroid cell-derived protein CNC homologous associated protein 1 can release Nrf2, which binds to the sequence of antioxidant response elements in the nucleus, hence having antioxidant effects. BLM could induce more severe PF in Nrf2 knockout mice compared with wild-type mice, supporting the protective role of Nrf2 against PF[50]. It has been reported that Nrf2 has a potential protective effect in human chronic fibrotic lung disease[51]. Zaafan *et al*[52] showed that amitriptyline attenuates PF through the inhibition of the NF-κB/TNF-α/TGF-β pathway, accompanied by a decrease in Nrf2 expression but its accumulation in nuclei. Considering that Nrf2 blocks the epithelial-to-mesenchymal transition in PF and regulates oxidative stress[53], the decreased Nrf2 expression is possibly a consequence of the less pro-fibrotic environment. In addition, its accumulation in the nuclei would increase the production of antioxidant proteins[54]. In the present study, the IHC results showed that the Nrf2 content in the lung tissue of the mice was significantly higher than in the sham group on day 28 after BLM modeling ($P < 0.05$) but significantly decreased after MSC-EVs treatment. However, there was no significant difference on day 14 after modeling. The results were consistent with those obtained by western blot. The lack of difference in Nrf2 on day 14 after treatment could be because the occurrence and development of PF is a chronic, progressive, evolutive process. Hence, because the process of PF is slow, the lung tissues on day 14 are in an acute or subacute inflammation phase, and the lung oxidative stress response has not been activated yet. On the other hand, on day 28, the development of PF reached a stage where oxidative stress was present, activating the Nrf2 antioxidant response. After MSC-EVs treatment, the oxidative stress environment in the lung was less severe, leading to a lower Nrf2 expression because of a weaker needed response. Of course, that hypothesis will have to be confirmed in future studies.

HO-1 is a key antioxidant enzyme widely present in various mammalian tissues and plays many key roles in the oxidation/antioxidant reactions *in vivo*. HO-1 can also play anti-inflammatory, antioxidant, and other physiological roles *in vivo*. It is the main downstream target of Nrf2[55]. Under normal circumstances, HO-1 expression is low *in vivo*, but its expression can be significantly increased by hypoxia, inflammation, and other factors that may induce oxidative stress [56]. Jin *et al*[57] concluded that the expression levels of HO-1 were significantly increased in the early stage of PF induced by BLM in experimental animals. Meanwhile, in our study, both *in vitro* and *in vivo* concluded that HO-1 expression levels were significantly increased at 14 and 28 d after BLM administration ($P < 0.05$), and MSC-EVs treatment could reverse the BLM-induced increase in the expression level of this molecule ($P < 0.05$). Therefore, MSC-EVs can alleviate the oxidative stress response of lung tissue by regulating Nrf2 and further regulating the expression of HO-1 in the development of PF and then improve PF.

IL-1β is a potent proinflammatory mediator activated by one of several inflammasome complexes, such as NLRP3, also known as Pyrin domain containing 3. Upon activation of this inflammasome, IL-1β is released, which was confirmed in chronic obstructive pulmonary disease, severe asthma, and respiratory infections[58]. The promoter region of the IL-1β gene contains the binding site of the NF-κB transcription factor, and the binding of NF-κB to this region activates the transcription of IL-1β. Thus, IL-1β expression is regulated by NF-κB[59]. NF-κB is an important target of the PTEN/PI3K/Akt pathway and regulates the secretion of various cytokines. In addition, NF-κB activation is also involved in the senescence process of various cells[60]. It is clear from previous studies on PF that inhibition of NF-κB signaling can inhibit the development of PF in BLM-induced PF model[61]. In the present study, *in vitro* and *in vivo* experiments showed that the expression of NF-κB and IL-1β was upregulated when PF occurred and downregulated after MSC-EVs

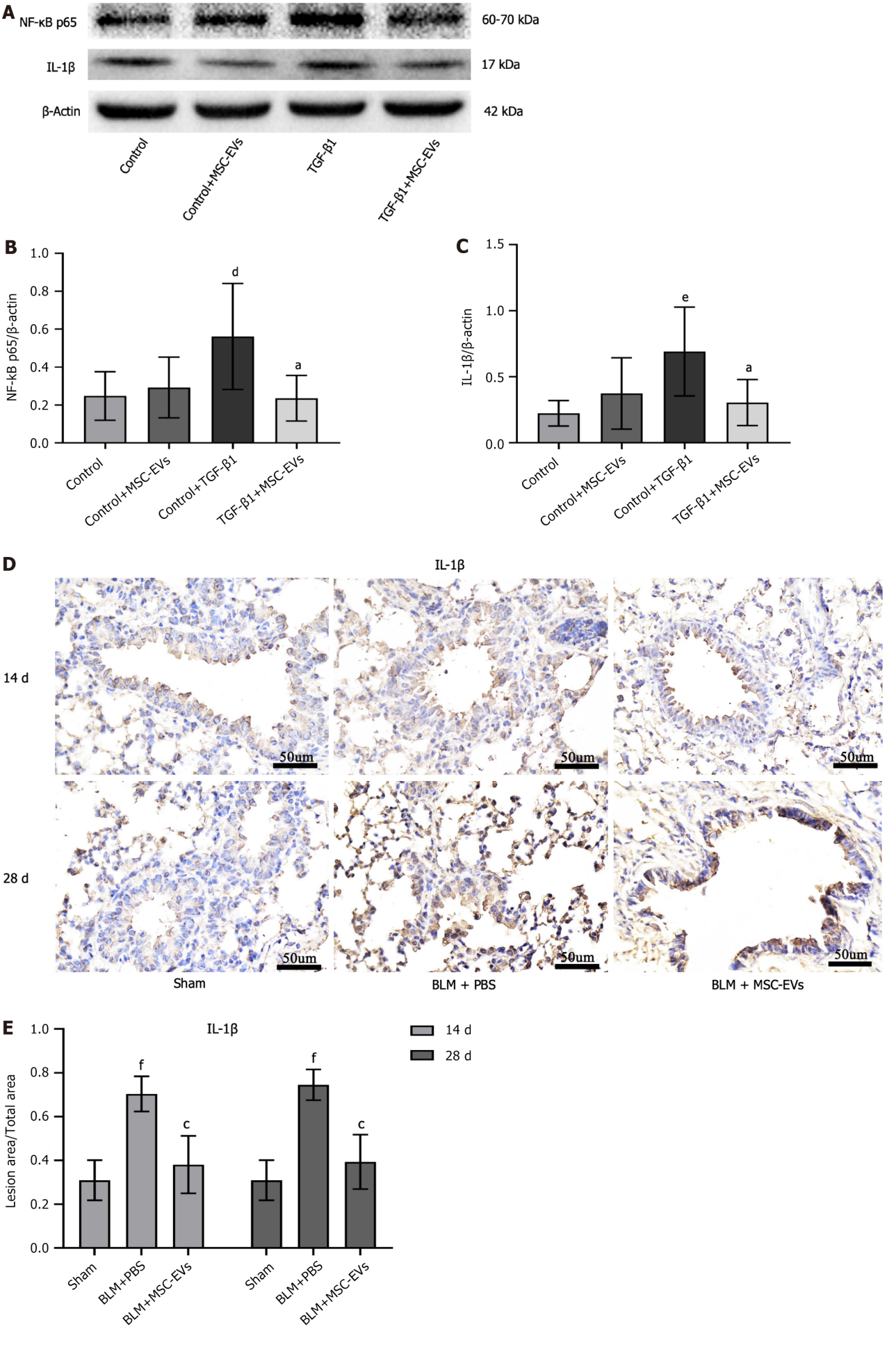
A
NF-κB p65
IL-1β
β-Actin
60-70 kDa
17 kDa
42 kDa
Control
Control+MSC-EVs
TGF-β1
TGF-β1+MSC-EVs
B
NF-kB p65/β-actin
1.0
0.8
0.6
0.4
0.2
0.0
d
a
Control
Control+MSC-EVs
Control+TGF-β1
TGF-β1+MSC-EVs
C
IL-1β/β-actin
1.5
1.0
0.5
0.0
e
a
Control
Control+MSC-EVs
Control+TGF-β1
TGF-β1+MSC-EVs
D
IL-1β
14 d
28 d
50um
Sham
BLM + PBS
BLM + MSC-EVs
E
IL-1β
14 d
28 d
Lesion area/Total area
1.0
0.8
0.6
0.4
0.2
0.0
f
c
f
c
Sham
BLM+PBS
BLM+MSC-EVs
Sham
BLM+PBS
BLM+MSC-EVs

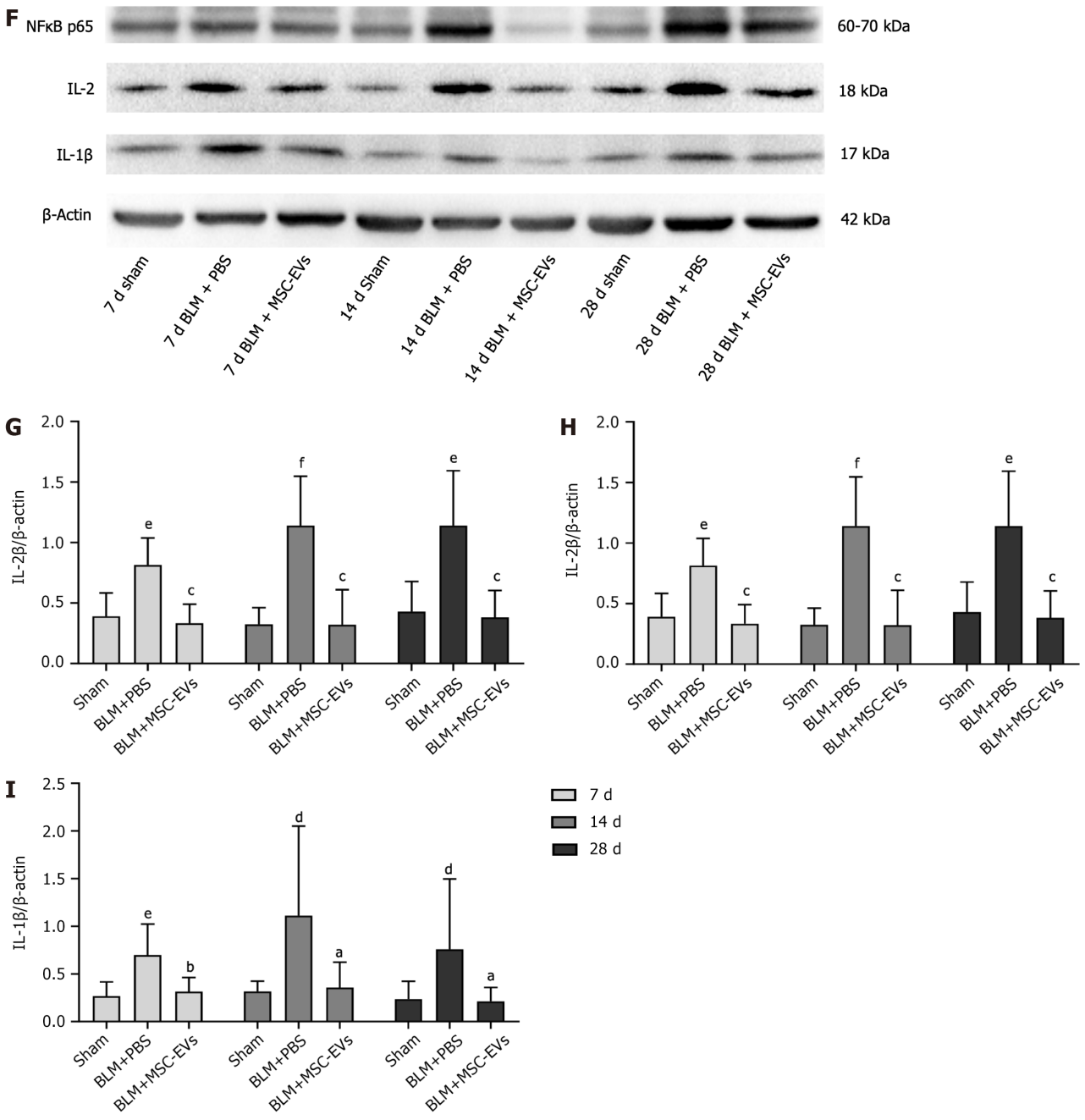

Figure 7 Mesenchymal stem cells-extracellular vesicles can inhibit the inflammatory response in the process of pulmonary fibrosis. A: The expressions of nuclear factor-kappaB (NF-κB) p65 and interleukin (IL)-1β in A549 cells of each group were verified by western blot; B and C: The statistical analysis of the expression levels of each protein. MSV-EVs can't induce an immune inflammatory response ($P > 0.05$). Transforming growth factor (TGF)-β can induce the immune inflammatory response of cells (NF-κB p65: $^{d}P < 0.05$ *vs* control group; IL-1β: $^{e}P < 0.01$ *vs* control group). However, mesenchymal stem cells-extracellular vesicles (MSC-EVs) can reverse the immune inflammatory response caused by TGF-β (NF-κB p65: $^{a}P < 0.05$; IL-1β: $^{a}P < 0.05$); D: The expression of IL-1β in lung tissue was observed by immunohistochemical (IHC) staining; E: The statistical analysis of the expression level of IL-1β in IHC staining. On day 14 and day 28, IL-1β (14 d: $^{f}P < 0.001$ *vs* sham group; 28 d: $^{f}P < 0.001$ *vs* sham group) deposition was observed in the bleomycin + phosphate buffered saline group, and the above pathological changes could be reversed after MSC-EVs treatment (14 d: $^{c}P < 0.001$; 28 d: $^{c}P < 0.001$); F: The western blot results of each protein's expression in mice's lung tissue in each group; G-I: The statistical analysis of western blot results of each protein in mouse lung tissue. No matter whether on day 7, 14, or 28, the expression of immune inflammatory response gene-related nuclear factor-kappaB (NF-κB) p65 (7 d: $^{d}P < 0.05$ *vs* sham group; 14 d: $^{e}P < 0.01$ *vs* sham group; 28 d: $^{d}P < 0.05$ *vs* sham group), IL-2 (7 d: $^{e}P < 0.01$ *vs* sham group; 14 d: $^{f}P < 0.001$ *vs* sham group; 28 d: $^{e}P < 0.01$ *vs* sham group) and IL-1β (7 d: $^{e}P < 0.01$ *vs* sham group; 14 d: $^{d}P < 0.05$ *vs* sham group; 28 d: $^{d}P < 0.05$ *vs* sham group) in lung tissue of mice was significantly higher than that in the sham group. After MSC-EVs treatment, the expression of NF-κB p65, IL-2, and IL-1β decreased significantly at 7 d (NF-κB p65: $^{a}P < 0.05$; IL-2: $^{c}P < 0.001$; IL-1β: $^{b}P < 0.01$) in the acute phase, 14 d in subacute phase (NF-κB p65: $^{b}P < 0.01$; IL-2: $^{c}P < 0.001$; IL-1β: $^{a}P < 0.05$) and 28 d in chronic phase (NF-κB p65: $^{a}P < 0.05$; IL-2: $^{c}P < 0.001$; IL-1β: $^{a}P < 0.05$). MSC: Mesenchymal stem cell; EV: Extracellular vesicle; BLM: Bleomycin; PBS: Phosphate buffered saline; TGF: Transforming growth factor; NF-κB: Nuclear factor-kappaB; IL: Interleukin.

treatment, indicating that MSC-EVs could significantly inhibit the inflammatory response in the process of PF.

CONCLUSION

BLM can induce PF *in vivo*, while TGF-β1 can induce PF *in vitro*. MSC-EVs can improve the EMT, oxidative stress response, and immune-inflammatory response during the development of PF. Through this experiment, based on further understanding of the occurrence and development mechanism of PF, the present study has shed some light on the role of MSC-EVs in PF. It can pave the way for new direction and theoretical basis for developing new treatment strategies.

Some limitations in this study were that it only verified the key molecules of the three main mechanisms of EMT, oxidative stress, and immune inflammatory response *in vitro* and *in vivo*, but did not knockdown or overexpress the important molecules of one of the pathways and verify the expression of upstream and downstream molecules, which is yet to be performed. In addition, the study was limited to establishing cell and experimental animal models and mechanism discussions and did not involve human specimens. Therefore, whether the results of this study can provide support for clinical trials is still lacking more precise evidence.

FOOTNOTES

Author contributions: Gao Y and Liu MF carried out the experiments, participated in the data collection, and drafted the manuscript; Li Y, Liu X, and Cao YJ performed the statistical analysis and participated in the study design; Long QF, Yu J, and Li JY helped draft the manuscript; and all authors read and approved the final manuscript.

Supported by Xi'an Science and Technology Plan Project, No. 20200001YX001(1); and Xi'an Talent Plan - Elite (Innovative Talents) Project, No. XAYC210062.

Institutional review board statement: This study was approved by the Ethics Committee guidelines of Xi'an Central Hospital, No. LW-2023-032.

Institutional animal care and use committee statement: All animal procedures were performed in accordance with the guidelines for the Care and Use of Laboratory Animals of the National Institutes of Health. All animal procedures were approved by the hospital's ethical committee for animals, No. IACUC-20210211.

Conflict-of-interest statement: All the authors report no relevant conflicts of interest for this article.

Data sharing statement: All data generated or analyzed during this study are included in this published article.

ARRIVE guidelines statement: The authors have read the ARRIVE guidelines, and the manuscript was prepared and revised according to the ARRIVE guidelines.

Country/Territory of origin: China

ORCID number: Jian-Ying Li 0009-0004-5485-9870.

S-Editor: Wang JJ
L-Editor: A
P-Editor: Zhang XD

REFERENCES

1 **Mei Q**, Liu Z, Zuo H, Yang Z, Qu J. Idiopathic Pulmonary Fibrosis: An Update on Pathogenesis. *Front Pharmacol* 2021; **12**: 797292 [PMID: 35126134 DOI: 10.3389/fphar.2021.797292]

2 **Richeldi L**, Rubin AS, Avdeev S, Udwadia ZF, Xu ZJ. Idiopathic pulmonary fibrosis in BRIC countries: the cases of Brazil, Russia, India, and China. *BMC Med* 2015; **13**: 237 [PMID: 26399999 DOI: 10.1186/s12916-015-0495-0]

3 **Ryerson CJ**, Urbania TH, Richeldi L, Mooney JJ, Lee JS, Jones KD, Elicker BM, Koth LL, King TE Jr, Wolters PJ, Collard HR. Prevalence and prognosis of unclassifiable interstitial lung disease. *Eur Respir J* 2013; **42**: 750-757 [PMID: 23222877 DOI: 10.1183/09031936.00131912]

4 **Martinez FJ**, Collard HR, Pardo A, Raghu G, Richeldi L, Selman M, Swigris JJ, Taniguchi H, Wells AU. Idiopathic pulmonary fibrosis. *Nat Rev Dis Primers* 2017; **3**: 17074 [PMID: 29052582 DOI: 10.1038/nrdp.2017.74]

5 **Mortimer KM**, Bartels DB, Hartmann N, Capapey J, Yang J, Gately R, Enger C. Characterizing Health Outcomes in Idiopathic Pulmonary

Fibrosis using US Health Claims Data. *Respiration* 2020; **99**: 108-118 [PMID: 31982886 DOI: 10.1159/000504630]

6 **Maher TM**, Bendstrup E, Dron L, Langley J, Smith G, Khalid JM, Patel H, Kreuter M. Global incidence and prevalence of idiopathic pulmonary fibrosis. *Respir Res* 2021; **22**: 197 [PMID: 34233665 DOI: 10.1186/s12931-021-01791-z]

7 **Raghu G**, Collard HR, Egan JJ, Martinez FJ, Behr J, Brown KK, Colby TV, Cordier JF, Flaherty KR, Lasky JA, Lynch DA, Ryu JH, Swigris JJ, Wells AU, Ancochea J, Bouros D, Carvalho C, Costabel U, Ebina M, Hansell DM, Johkoh T, Kim DS, King TE Jr, Kondoh Y, Myers J, Müller NL, Nicholson AG, Richeldi L, Selman M, Dudden RF, Griss BS, Protzko SL, Schünemann HJ; ATS/ERS/JRS/ALAT Committee on Idiopathic Pulmonary Fibrosis. An official ATS/ERS/JRS/ALAT statement: idiopathic pulmonary fibrosis: evidence-based guidelines for diagnosis and management. *Am J Respir Crit Care Med* 2011; **183**: 788-824 [PMID: 21471066 DOI: 10.1164/rccm.2009-040GL]

8 **Yu QY**, Tang XX. Irreversibility of Pulmonary Fibrosis. *Aging Dis* 2022; **13**: 73-86 [PMID: 35111363 DOI: 10.14336/AD.2021.0730]

9 **Wynn TA**. Integrating mechanisms of pulmonary fibrosis. *J Exp Med* 2011; **208**: 1339-1350 [PMID: 21727191 DOI: 10.1084/jem.20110551]

10 **Lamas DJ**, Kawut SM, Bagiella E, Philip N, Arcasoy SM, Lederer DJ. Delayed access and survival in idiopathic pulmonary fibrosis: a cohort study. *Am J Respir Crit Care Med* 2011; **184**: 842-847 [PMID: 21719755 DOI: 10.1164/rccm.201104-0668OC]

11 **Aburto M**, Herráez I, Iturbe D, Jiménez-Romero A. Diagnosis of Idiopathic Pulmonary Fibrosis: Differential Diagnosis. *Med Sci (Basel)* 2018; **6** [PMID: 30181506 DOI: 10.3390/medsci6030073]

12 **Lynch DA**, Sverzellati N, Travis WD, Brown KK, Colby TV, Galvin JR, Goldin JG, Hansell DM, Inoue Y, Johkoh T, Nicholson AG, Knight SL, Raoof S, Richeldi L, Ryerson CJ, Ryu JH, Wells AU. Diagnostic criteria for idiopathic pulmonary fibrosis: a Fleischner Society White Paper. *Lancet Respir Med* 2018; **6**: 138-153 [PMID: 29154106 DOI: 10.1016/S2213-2600(17)30433-2]

13 **Khan MA**, Sherbini N, Alyami S, Al-Harbi A, Al-Ghamdi M, Alrajhi S, Rajendram R, Al-Jahdali H. Nintedanib and pirfenidone for idiopathic pulmonary fibrosis in King Abdulaziz Medical City, Riyadh: Real-life data. *Ann Thorac Med* 2023; **18**: 45-51 [PMID: 36968327 DOI: 10.4103/atm.atm_206_22]

14 **Flaherty KR**, Fell CD, Huggins JT, Nunes H, Sussman R, Valenzuela C, Petzinger U, Stauffer JL, Gilberg F, Bengus M, Wijsenbeek M. Safety of nintedanib added to pirfenidone treatment for idiopathic pulmonary fibrosis. *Eur Respir J* 2018; **52** [PMID: 29946005 DOI: 10.1183/13993003.00230-2018]

15 **Laporta Hernandez R**, Aguilar Perez M, Lázaro Carrasco MT, Ussetti Gil P. Lung Transplantation in Idiopathic Pulmonary Fibrosis. *Med Sci (Basel)* 2018; **6** [PMID: 30142942 DOI: 10.3390/medsci6030068]

16 **Squillaro T**, Peluso G, Galderisi U. Clinical Trials With Mesenchymal Stem Cells: An Update. *Cell Transplant* 2016; **25**: 829-848 [PMID: 26423725 DOI: 10.3727/096368915X689622]

17 **Ryu JS**, Jeong EJ, Kim JY, Park SJ, Ju WS, Kim CH, Kim JS, Choo YK. Application of Mesenchymal Stem Cells in Inflammatory and Fibrotic Diseases. *Int J Mol Sci* 2020; **21** [PMID: 33171878 DOI: 10.3390/ijms21218366]

18 **Tzouvelekis A**, Toonkel R, Karampitsakos T, Medapalli K, Ninou I, Aidinis V, Bouros D, Glassberg MK. Mesenchymal Stem Cells for the Treatment of Idiopathic Pulmonary Fibrosis. *Front Med (Lausanne)* 2018; **5**: 142 [PMID: 29868594 DOI: 10.3389/fmed.2018.00142]

19 **Wei L**, Zhang J, Yang ZL, You H. Extracellular superoxide dismutase increased the therapeutic potential of human mesenchymal stromal cells in radiation pulmonary fibrosis. *Cytotherapy* 2017; **19**: 586-602 [PMID: 28314668 DOI: 10.1016/j.jcyt.2017.02.359]

20 **Liu D**, Kong F, Yuan Y, Seth P, Xu W, Wang H, Xiao F, Wang L, Zhang Q, Yang Y. Decorin-Modified Umbilical Cord Mesenchymal Stem Cells (MSCs) Attenuate Radiation-Induced Lung Injuries *via* Regulating Inflammation, Fibrotic Factors, and Immune Responses. *Int J Radiat Oncol Biol Phys* 2018; **101**: 945-956 [PMID: 29976507 DOI: 10.1016/j.ijrobp.2018.04.007]

21 **Rong X**, Yang Y, Zhang G, Zhang H, Li C, Wang Y. Antler stem cells as a novel stem cell source for reducing liver fibrosis. *Cell Tissue Res* 2020; **379**: 195-206 [PMID: 31428875 DOI: 10.1007/s00441-019-03081-z]

22 **Roura S**, Gálvez-Montón C, Mirabel C, Vives J, Bayes-Genis A. Mesenchymal stem cells for cardiac repair: are the actors ready for the clinical scenario? *Stem Cell Res Ther* 2017; **8**: 238 [PMID: 29078809 DOI: 10.1186/s13287-017-0695-y]

23 **Lalit PA**, Hei DJ, Raval AN, Kamp TJ. Induced pluripotent stem cells for post-myocardial infarction repair: remarkable opportunities and challenges. *Circ Res* 2014; **114**: 1328-1345 [PMID: 24723658 DOI: 10.1161/CIRCRESAHA.114.300556]

24 **Chang D**, Yang X, Fan S, Fan T, Zhang M, Ono M. Engineering of MSCs sheet for the prevention of myocardial ischemia and for left ventricle remodeling. *Stem Cell Res Ther* 2023; **14**: 102 [PMID: 37098611 DOI: 10.1186/s13287-023-03322-7]

25 **Qiu H**, Liu S, Wu K, Zhao R, Cao L, Wang H. Prospective application of exosomes derived from adipose-derived stem cells in skin wound healing: A review. *J Cosmet Dermatol* 2020; **19**: 574-581 [PMID: 31755172 DOI: 10.1111/jocd.13215]

26 **Pu CM**, Liu CW, Liang CJ, Yen YH, Chen SH, Jiang-Shieh YF, Chien CL, Chen YC, Chen YL. Adipose-Derived Stem Cells Protect Skin Flaps against Ischemia/Reperfusion Injury *via* IL-6 Expression. *J Invest Dermatol* 2017; **137**: 1353-1362 [PMID: 28163069 DOI: 10.1016/j.jid.2016.12.030]

27 **Duan M**, Zhang Y, Zhang H, Meng Y, Qian M, Zhang G. Epidermal stem cell-derived exosomes promote skin regeneration by downregulating transforming growth factor-β1 in wound healing. *Stem Cell Res Ther* 2020; **11**: 452 [PMID: 33097078 DOI: 10.1186/s13287-020-01971-6]

28 **Fu J**, Wang Y, Jiang Y, Du J, Xu J, Liu Y. Systemic therapy of MSCs in bone regeneration: a systematic review and meta-analysis. *Stem Cell Res Ther* 2021; **12**: 377 [PMID: 34215342 DOI: 10.1186/s13287-021-02456-w]

29 **Huang J**, Liu Q, Xia J, Chen X, Xiong J, Yang L, Liang Y. Modification of mesenchymal stem cells for cartilage-targeted therapy. *J Transl Med* 2022; **20**: 515 [PMID: 36348497 DOI: 10.1186/s12967-022-03726-8]

30 **El Agha E**, Kramann R, Schneider RK, Li X, Seeger W, Humphreys BD, Bellusci S. Mesenchymal Stem Cells in Fibrotic Disease. *Cell Stem Cell* 2017; **21**: 166-177 [PMID: 28777943 DOI: 10.1016/j.stem.2017.07.011]

31 **Qin L**, Liu N, Bao CL, Yang DZ, Ma GX, Yi WH, Xiao GZ, Cao HL. Mesenchymal stem cells in fibrotic diseases-the two sides of the same coin. *Acta Pharmacol Sin* 2023; **44**: 268-287 [PMID: 35896695 DOI: 10.1038/s41401-022-00952-0]

32 **Stolzing A**, Jones E, McGonagle D, Scutt A. Age-related changes in human bone marrow-derived mesenchymal stem cells: consequences for cell therapies. *Mech Ageing Dev* 2008; **129**: 163-173 [PMID: 18241911 DOI: 10.1016/j.mad.2007.12.002]

33 **Baksh D**, Yao R, Tuan RS. Comparison of proliferative and multilineage differentiation potential of human mesenchymal stem cells derived from umbilical cord and bone marrow. *Stem Cells* 2007; **25**: 1384-1392 [PMID: 17332507 DOI: 10.1634/stemcells.2006-0709]

34 **Rani S**, Ryan AE, Griffin MD, Ritter T. Mesenchymal Stem Cell-derived Extracellular Vesicles: Toward Cell-free Therapeutic Applications. *Mol Ther* 2015; **23**: 812-823 [PMID: 25868399 DOI: 10.1038/mt.2015.44]

35 **Shi L**, Ren J, Li J, Wang D, Wang Y, Qin T, Li X, Zhang G, Li C. Extracellular vesicles derived from umbilical cord mesenchymal stromal cells alleviate pulmonary fibrosis by means of transforming growth factor-β signaling inhibition. *Stem Cell Res Ther* 2021; **12**: 230 [PMID: 33845892 DOI: 10.1186/s13287-021-02296-8]

36 **Leung J**, Cho Y, Lockey RF, Kolliputi N. The Role of Aging in Idiopathic Pulmonary Fibrosis. *Lung* 2015; **193**: 605-610 [PMID: 25903793 DOI: 10.1007/s00408-015-9729-3]

37 **Selman M**, Pardo A. Revealing the pathogenic and aging-related mechanisms of the enigmatic idiopathic pulmonary fibrosis. an integral model. *Am J Respir Crit Care Med* 2014; **189**: 1161-1172 [PMID: 24641682 DOI: 10.1164/rccm.201312-2221PP]

38 **Bagnato G**, Harari S. Cellular interactions in the pathogenesis of interstitial lung diseases. *Eur Respir Rev* 2015; **24**: 102-114 [PMID: 25726561 DOI: 10.1183/09059180.00003214]

39 Guide for the Care and Use of Laboratory Animals. Washington (DC): National Academies Press (US); 2011– [PMID: 21595115]

40 **Xian P**, Hei Y, Wang R, Wang T, Yang J, Li J, Di Z, Liu Z, Baskys A, Liu W, Wu S, Long Q. Mesenchymal stem cell-derived exosomes as a nanotherapeutic agent for amelioration of inflammation-induced astrocyte alterations in mice. *Theranostics* 2019; **9**: 5956-5975 [PMID: 31534531 DOI: 10.7150/thno.33872]

41 **Choi MR**, Kim HY, Park JY, Lee TY, Baik CS, Chai YG, Jung KH, Park KS, Roh W, Kim KS, Kim SH. Selection of optimal passage of bone marrow-derived mesenchymal stem cells for stem cell therapy in patients with amyotrophic lateral sclerosis. *Neurosci Lett* 2010; **472**: 94-98 [PMID: 20117176 DOI: 10.1016/j.neulet.2010.01.054]

42 **Wang T**, Jian Z, Baskys A, Yang J, Li J, Guo H, Hei Y, Xian P, He Z, Li Z, Li N, Long Q. MSC-derived exosomes protect against oxidative stress-induced skin injury *via* adaptive regulation of the NRF2 defense system. *Biomaterials* 2020; **257**: 120264 [PMID: 32791387 DOI: 10.1016/j.biomaterials.2020.120264]

43 **Yildirim M**, Oztay F, Kayalar O, Tasci AE. Effect of long noncoding RNAs on epithelial-mesenchymal transition in A549 cells and fibrotic human lungs. *J Cell Biochem* 2021; **122**: 882-896 [PMID: 33847014 DOI: 10.1002/jcb.29920]

44 **Wang D**, Yan Z, Bu L, An C, Deng B, Zhang J, Rao J, Cheng L, Zhang B, Xie J. Protective effect of peptide DR8 on bleomycin-induced pulmonary fibrosis by regulating the TGF-β/MAPK signaling pathway and oxidative stress. *Toxicol Appl Pharmacol* 2019; **382**: 114703 [PMID: 31398421 DOI: 10.1016/j.taap.2019.114703]

45 **Liu T**, Ullenbruch M, Young Choi Y, Yu H, Ding L, Xaubet A, Pereda J, Feghali-Bostwick CA, Bitterman PB, Henke CA, Pardo A, Selman M, Phan SH. Telomerase and telomere length in pulmonary fibrosis. *Am J Respir Cell Mol Biol* 2013; **49**: 260-268 [PMID: 23526226 DOI: 10.1165/rcmb.2012-0514OC]

46 **Tang Z**, Gao J, Wu J, Zeng G, Liao Y, Song Z, Liang X, Hu J, Hu Y, Liu M, Li N. Human umbilical cord mesenchymal stromal cells attenuate pulmonary fibrosis *via* regulatory T cell through interaction with macrophage. *Stem Cell Res Ther* 2021; **12**: 397 [PMID: 34256845 DOI: 10.1186/s13287-021-02469-5]

47 **Kim KK**, Dotson MR, Agarwal M, Yang J, Bradley PB, Subbotina N, Osterholzer JJ, Sisson TH. Efferocytosis of apoptotic alveolar epithelial cells is sufficient to initiate lung fibrosis. *Cell Death Dis* 2018; **9**: 1056 [PMID: 30333529 DOI: 10.1038/s41419-018-1074-z]

48 **Mi S**, Li Z, Yang HZ, Liu H, Wang JP, Ma YG, Wang XX, Liu HZ, Sun W, Hu ZW. Blocking IL-17A promotes the resolution of pulmonary inflammation and fibrosis *via* TGF-beta1-dependent and -independent mechanisms. *J Immunol* 2011; **187**: 3003-3014 [PMID: 21841134 DOI: 10.4049/jimmunol.1004081]

49 **Amara N**, Goven D, Prost F, Muloway R, Crestani B, Boczkowski J. NOX4/NADPH oxidase expression is increased in pulmonary fibroblasts from patients with idiopathic pulmonary fibrosis and mediates TGFbeta1-induced fibroblast differentiation into myofibroblasts. *Thorax* 2010; **65**: 733-738 [PMID: 20685750 DOI: 10.1136/thx.2009.113456]

50 **Cho HY**, Reddy SP, Yamamoto M, Kleeberger SR. The transcription factor NRF2 protects against pulmonary fibrosis. *FASEB J* 2004; **18**: 1258-1260 [PMID: 15208274 DOI: 10.1096/fj.03-1127fje]

51 **Mazur W**, Lindholm P, Vuorinen K, Myllärniemi M, Salmenkivi K, Kinnula VL. Cell-specific elevation of NRF2 and sulfiredoxin-1 as markers of oxidative stress in the lungs of idiopathic pulmonary fibrosis and non-specific interstitial pneumonia. *APMIS* 2010; **118**: 703-712 [PMID: 20718723 DOI: 10.1111/j.1600-0463.2010.02646.x]

52 **Zaafan MA**, Haridy AR, Abdelhamid AM. Amitriptyline attenuates bleomycin-induced pulmonary fibrosis: modulation of the expression of NF-κβ, iNOS, and Nrf2. *Naunyn Schmiedebergs Arch Pharmacol* 2019; **392**: 279-286 [PMID: 30474696 DOI: 10.1007/s00210-018-1586-1]

53 **Zhang Z**, Qu J, Zheng C, Zhang P, Zhou W, Cui W, Mo X, Li L, Xu L, Gao J. Nrf2 antioxidant pathway suppresses Numb-mediated epithelial-mesenchymal transition during pulmonary fibrosis. *Cell Death Dis* 2018; **9**: 83 [PMID: 29362432 DOI: 10.1038/s41419-017-0198-x]

54 **Kikuchi N**, Ishii Y, Morishima Y, Yageta Y, Haraguchi N, Itoh K, Yamamoto M, Hizawa N. Nrf2 protects against pulmonary fibrosis by regulating the lung oxidant level and Th1/Th2 balance. *Respir Res* 2010; **11**: 31 [PMID: 20298567 DOI: 10.1186/1465-9921-11-31]

55 **Nakamura T**, Matsushima M, Hayashi Y, Shibasaki M, Imaizumi K, Hashimoto N, Shimokata K, Hasegawa Y, Kawabe T. Attenuation of transforming growth factor-β-stimulated collagen production in fibroblasts by quercetin-induced heme oxygenase-1. *Am J Respir Cell Mol Biol* 2011; **44**: 614-620 [PMID: 21216973 DOI: 10.1165/rcmb.2010-0338OC]

56 **Haines DD**, Lekli I, Teissier P, Bak I, Tosaki A. Role of haeme oxygenase-1 in resolution of oxidative stress-related pathologies: focus on cardiovascular, lung, neurological and kidney disorders. *Acta Physiol (Oxf)* 2012; **204**: 487-501 [PMID: 22118298 DOI: 10.1111/j.1748-1716.2011.02387.x]

57 **Jin C**, Zhou D, Lv F. Beneficial effects of early (but not late) intervention of heme oxygenase-1 on bleomycin-induced pulmonary fibrosis in mice. *Respir Physiol Neurobiol* 2011; **175**: 239-246 [PMID: 21111848 DOI: 10.1016/j.resp.2010.11.010]

58 **Pinkerton JW**, Kim RY, Robertson AAB, Hirota JA, Wood LG, Knight DA, Cooper MA, O'Neill LAJ, Horvat JC, Hansbro PM. Inflammasomes in the lung. *Mol Immunol* 2017; **86**: 44-55 [PMID: 28129896 DOI: 10.1016/j.molimm.2017.01.014]

59 **Hu J**, Wang H, Li X, Liu Y, Mi Y, Kong H, Xi D, Yan W, Luo X, Ning Q, Wang X. Fibrinogen-like protein 2 aggravates nonalcoholic steatohepatitis *via* interaction with TLR4, eliciting inflammation in macrophages and inducing hepatic lipid metabolism disorder. *Theranostics* 2020; **10**: 9702-9720 [PMID: 32863955 DOI: 10.7150/thno.44297]

60 **Tian Y**, Li H, Qiu T, Dai J, Zhang Y, Chen J, Cai H. Loss of PTEN induces lung fibrosis *via* alveolar epithelial cell senescence depending on NF-κB activation. *Aging Cell* 2019; **18**: e12858 [PMID: 30548445 DOI: 10.1111/acel.12858]

61 **Hou J**, Ma T, Cao H, Chen Y, Wang C, Chen X, Xiang Z, Han X. TNF-α-induced NF-κB activation promotes myofibroblast differentiation of LR-MSCs and exacerbates bleomycin-induced pulmonary fibrosis. *J Cell Physiol* 2018; **233**: 2409-2419 [PMID: 28731277 DOI: 10.1002/jcp.26112]

Published by **Baishideng Publishing Group Inc**
7041 Koll Center Parkway, Suite 160, Pleasanton, CA 94566, USA
Telephone: +1-925-3991568
E-mail: office@baishideng.com
Help Desk: https://www.f6publishing.com/helpdesk
https://www.wjgnet.com